



1 **Influence of initial soil moisture in a Regional**
2 **Climate Model study over West Africa: Part 1:**
3 **Impact on the climate mean.**

4
5 Brahima KONÉ¹, Arona DIEDHIOU^{1, 2}, Adama Diawara¹, Sandrine Anquetin², N'datchoh
6 Evelyne Touré¹, Adama Bamba¹, and Arsene Toka Koba¹

7 ¹LAPAMF, Université Félix Houphouët Boigny, Abidjan, Côte d'Ivoire

8 ²Univ. Grenoble Alpes, IRD, CNRS, Grenoble INP, IGE, F-38000 Grenoble, France

9 *Correspondence to:* Arona DIEDHIOU (arona.diedhiou@ird.fr)

10 **Abstract.**

11 The impact of the anomalies in initial soil moisture in later spring on the subsequent mean
12 climate over West Africa is examined using the latest version of Regional Climate Model of
13 the International Centre for Theoretical Physics (RegCM4). We performed this sensitivity
14 studies over the West African domain, for June-July-August-September (JJAS) 2003 (wet year)
15 and JJAS 2004 (a dry year) at the horizontal resolution of 25 km × 25 km. The reanalysis soil
16 moisture of the European Centre Meteorological Weather Forecast's reanalysis of the 20th
17 century (ERA20C) were used to initialize the control runs, whereas we initialized the soil
18 moisture at the wilting points and field capacity respectively in dry and wet experiments. The
19 impact of the anomalies in initial soil moisture on the precipitation in West Africa is
20 homogeneous only over the central Sahel where dry (wet) experiments lead to rainfall decrease
21 (increase). The strongest impact on precipitation in wet and dry experiments is found
22 respectively over west and central Sahel with the peak of change about respectively 40% and -
23 8%. The impact of the anomalies in initial soil moisture can persist for three or even four
24 months, however the significance influence on precipitation, greater than 1mm.day⁻¹, of the
25 impact of the anomalies in initial soil moisture is much shorter, no longer than one month. The
26 effect of soil moisture anomalies is mostly confined to the near-surface climate and in the upper
27 troposphere. Overall, the impact of the anomalies in initial soil moisture is greater on
28 temperature than on precipitation over most areas studied. The strongest homogeneous impacts
29 of the anomalies in initial soil moisture on temperature is located over the central Sahel with
30 the peak of change at -1.5 °C and 0.5°C respectively in wet and dry experiments. The influence
31 of initial the anomalies in initial soil moisture on the precipitation mechanism is also



32 highlighted. We will investigate in the Part II of this study the influence of the anomalies in
33 initial soil moisture on climate extremes.

34 **1 Introduction**

35 In the climate system soil moisture is one of the crucial variables which influence water balance
36 and surface energy components through latent surface fluxes and evaporation. Therefore, soil
37 moisture impacts the development of weather patterns and precipitation production. The
38 strength of soil moisture impact on land-atmosphere coupling is variable according to the place
39 and with season. Koster et al. (2004) sustained that the atmospheric response simulation to the
40 slow variation of the ocean and land surface states, can accurate the seasonal simulations. The
41 atmosphere response to ocean temperature anomalies is well documented (Kirtman and al.
42 1998; Rasmusson and al.1982). Another earth system component, potentially useful, that varies
43 slowly is soil moisture. The role of the soils may be comparable to that of the oceans. While in
44 summer, the solar energy received by the oceans is stored (and use it to heat the atmosphere in
45 winter), in winter the precipitation received by the soil is stored (the moistening and cooling is
46 return to the atmosphere in summer). Through its impact on surface energy fluxes and
47 evaporation, there are many additional impacts on climate process of soil moisture, such as
48 boundary-layer stability and air temperature (Hong and al., 2000; Kim and Hong 2007). Several
49 studies shown that, the anomalies of the soil moisture may persist for several weeks or months,
50 however, its impact remains only for shorter time in the atmosphere, not exceed few days
51 (Vinnikov and Yeserkepova 1991; Liu and al., 2014). The important role of the anomalies in
52 soil moisture in coupling of land and atmosphere is shown in several studies, using numerical
53 climate models (Jaeger and al., 2011; Zhang and al., 2011) and observation datasets (Zhang et
54 al., 2008a; Dirmeyer et al., 2006).

55 West Africa known to be a region where there is a strong coupling between soil moisture and
56 precipitation (Koster et al., 2004). Several previous studies have been conducted over West
57 Africa on a global scale using AGCMs (Atmospheric General Circulation Model) to investigate
58 the impact on land-atmosphere coupling of soil moisture anomalies (Koster and al., 2004;
59 Douville and al, 2001; Zhang and al., 2008b). However at the local and regional scales, the
60 land-atmosphere coupling studies with AGCM, present large uncertainties (Xue et al. 2010).
61 Recently, the use of RCMs to simulate the impact on interannual climate variability of
62 anomalies in soil moisture received a lot of attention because of the increase in climate
63 variability associated with extreme weather events that can have greater societal and
64 environmental impacts. In general, these studies have been conducted for Asia, Europe and



65 America (e.g. Seneviratne and al. 2006 for Europe; Zhang and al. 2011 for Asia; Zhang and al.
66 2008b for America). Overall, the results of these studies show, during summertime, the strong
67 impact of the anomalies of soil moisture in land-atmosphere occurred mainly over the transition
68 zones with a climate between wet and dry climate regimes. The relevance and extent of this
69 potential feedback are still poorly understood over the West Africa. This study will focus on
70 the influence of initial soil moisture anomalies on climate mean and it is based on performance
71 assessment of the Regional Climate model version 4 coupled to the version 4.5 of the
72 Community Land Model (RegCM4-CLM4.5) done by Koné and al. (2018) where the ability of
73 the model to reproduce the climate mean has been validated. While in the part II of the article,
74 the influence of soil moisture on climate extremes will be explored. The descriptions of the
75 model and experiment setup used in this study are presented in Section. 2; in the Section 3, the
76 influence of the anomalies in initial soil moisture on the subsequent climate mean is analyzed
77 and discussed; and in Section 4 the main conclusions close the paper.

78 **2. Model and experimental design**

79 **2.1 Descriptions of the model and the observed datasets**

80 We used in this study, the fourth generation of the Regional Climate Model (RegCM4) of the
81 International Centre for Theoretical Physics (ICTP). Since this release, the physical
82 representations have been submitted to a continuous process of development and
83 implementation. The version used in the present study is RegCM4.7. The MM5 (Grell et al.,
84 1994) non-hydrostatic dynamical core has been ported to RegCM without removing the existing
85 hydrostatic core. The model dynamical core used in this study is the non-hydrostatic. RegCM4
86 is a limited area model using a sigma pressure vertical grid and the finite differencing algorithm
87 of Arakawa B-grid (Giorgi and al., 2012). The radiation scheme used in this version of
88 RegCM4.7 is derived from NCAR (National Center for Atmospheric Research) Community
89 Climate Model Version 3 (CCM3) (Kiehl and al., 1996), the representation of aerosols is from
90 Zakey and al. (2006) and Solmon and al. (2006). The scheme of the large-scale precipitation
91 used is from Pal and al. (2000), the moisture scheme is the SUBEX (SUBgrid EXplicit moisture
92 scheme) takes in account the cloud variability scale sub-grid, and the accretion processes and
93 evaporation for stable precipitation following the work of Sundqvist and al., 1989. In planetary
94 boundary layer, the sensible heat over ocean and land, the water vapor and the turbulent
95 transports of momentum are calculated according to the scheme of Holtslag and al. (1990). The
96 heat and moisture, the momentum fluxes of ocean surfaces in this study are computed as in
97 Zeng and al. (1998). In RegCM4.7, convective precipitation and the land surface processes can



98 be described by several parameterizations. Based on Koné and al. (2018), we selected the
99 convective scheme of Emanuel (Emanuel, 1991) and the interaction processes between soil,
100 vegetation and atmosphere are parameterized with CLM4.5. In each grid cell, CLM4.5 has 16
101 different PFTs (Plant functional Types) and 10 soil layers (Lawrence et al., 2011; Wang and
102 al., 2016). RegCM4 was integrated over the domain of West Africa depicted in Fig. 1 with 25
103 km of horizontal resolution and with 18 vertical levels and the initial and boundary conditions
104 are from the European Centre for Medium-Range Weather Forecasts reanalysis (EIN75; Uppala
105 and al., 2008; Simmons and al., 2007). The Sea Surface Temperatures (SST) is from the
106 National Oceanic and Atmosphere Administration (NOAA) optimal interpolation weekly
107 (OI_WK) (Reynolds and al., 1996). The source for the topography is from States Geological
108 Survey (USGS) Global Multi-resolution Terrain Elevation Data (GMTED; Danielson and al.,
109 2011) at 30 arc-second spatial resolution which is an update to the Global Land Cover
110 Characterization (GTOPO; Loveland and al., 2000) dataset.

111 Our analysis is focused on the precipitation and the 2m air temperature over the West African
112 domain during the summer of June-July-August-September (JJAS) for 2003 and 2004. The
113 uncertainties reduction related to the absence of reliable observation system over the region
114 (Sylla et al., 2013a; Nikulin et al., 2012), we validated the simulated precipitation based on two
115 products : the TRMM datasets (Tropical Rainfall Measuring Mission 3B43V7) at the high-
116 resolution 0.25° , available from 1998 to 2013 (Huffman and al., 2007), and The Climate
117 Hazards group Infrared Precipitation with Stations (CHIRPS) dataset developed at the
118 University of California at Santa Barbara at the 0.05° high-resolution available from 1981 to
119 2020. The validation of the simulated 2 m temperature relies on two observational datasets: the
120 global daily temperature from the Global Telecommunication System (hereafter GTS), gridded
121 at 0.5° of horizontal resolution for 1979 to 2020 (Fan and van den Dool, 2008) and the CRU
122 datasets (Climate Research Unit version 3.20) from the University of East Anglia, gridded at
123 the horizontal resolution 0.5° and available from 1901 to 2011 (Harris et al., 2013). To facilitate
124 the comparison with RegCM4 simulations, all products are re-gridded to $0.22^\circ \times 0.22^\circ$ using a
125 method of bilinear interpolation (Nikulin et al., 2012).

126

127 **2.2 Experiments setup and analysis methodology**

128 It is known that sensitivity of initial soil moisture is no longer than one season. That's why
129 Hong and Pan (2000) use in their study only two years (3 months per year) to investigate the
130 impact of initial soil moisture over the North of America (in the Great Plains) during the two



131 summers, May-June-July (MJJ) 1988 (corresponding to a drought season) and MJJ 1993
132 (correspond to an extreme wet season). Over Asia also, Kim and Hong (2006) used in their
133 study two contrasted years (1997 and 1998, 4 months per year). In this study, the two years
134 2003 and 2004 have been chosen because they correspond respectively to a wet and dry year in
135 the region of interest. The simulations start from June 1st and span four months, JJAS 2003 and
136 JJAS 2004, and the results during the first 7 days (Kang and al., 2014) are excluded in the
137 analysis as a spin-up period.

138 With very little variation in soil moisture in one day, initial soil moisture anomalies are given
139 at the first step of June 1st for the two summers JJAS 2003 and JJAS 2004. Except for the
140 geographical location, the experimental setup is the same as that of Hong and al. (2000). The
141 geographical location of this study is the same as in Koné et al (2018), with four sub-regions,
142 each with different features of annual cycle of precipitation (Fig. 1). For each year, three
143 experiments are conducted; we used the soil moisture from the reanalysis of the European
144 Centre Meteorological Weather Forecast's reanalysis of the 20th century (ERA20C) to initialize
145 the control runs. We initialized the dry and wet soil moisture (in volumetric fraction $\text{m}^3 \cdot \text{m}^{-3}$)
146 respectively at the wilting point ($=0.117 \cdot 10^{-4}$) and the field capacity ($=0.489$) derived from
147 ERA20C dataset.

148 Generally, in several previous studies (Liu and al. (2014), Hong and al. (2000), Kim and Hong
149 (2006)), the analysis methodology used is the mean biases (MB) averaged over their domains
150 studied to quantify the impact of soil moisture anomalies, while in our study we used the mean
151 biases and the probability density function (PDF, Gao et al. 2016; Jaeger and Seneviratne 2011)
152 by fitting a normal distribution for this purpose to better capture how many grid points are
153 impacted by the anomalies in initial soil moisture. The pattern correlation coefficient (PCC) is
154 also used as spatial correlation to reveal the degree of large-scale similarity between model
155 simulations and the observation. We used the two-tailed t-test to investigate the differences
156 which are statistically significant at each grid cell between the control and the wet and dry
157 sensitivity experiments.

158

159 **3. Results and discussion**

160 **3.1. Influence of initial soil moisture anomalies on precipitation.**

161 Fig.2 displays the spatial distribution of observed mean rainfall (mm/day) from CHIRPS
162 (Fig.2a, d) and TRMM (Fig.2b, e) for JJAS 2003 and JJAS 2004 and their corresponding
163 simulated from control experiments (Fig.2c, f) initialized with reanalysis soil moisture



164 ERA20C. Table 1 reports the MB and the PCC for the simulations of the model and TRMM
165 observation compared to CHIRPS, computed for central Sahel, Guinea coast, west Sahel and
166 the entire West African domain. CHIRPS product displays a zonal band of rainfall centered
167 around 10° N decreasing from north to south (Fig.2a, d). The maximum values are located over
168 the mountain regions of Cameroun and Guinea. The TRMM observation (Fig.2b, e) is closer to
169 CHIRPS, and represents quite similarly the North–South gradient of precipitation with PCC up
170 to 0.97 over the entire West African domain for both JJAS 2003 and JJAS 2004 (Table 1).
171 However, although the observation datasets have similar large-scale patterns, they present
172 differences at the local scale. CHIRPS shows a much larger extend of these maxima than
173 TRMM, especially over the Guinea highland and Cameroon mountains, while TRMM shows a
174 large band of precipitation which extend too far into the Sahel region. The strongest mean bias
175 between the two products is dryer about -15.45 and -16.96 % respectively for JJAS 2003 and
176 JJAS 2004, and it is found over the Guinea coast sub-region (Table 1). The control experiments
177 (Fig.2 c and f) initialized with the reanalyze ERA20C soil moisture well reproduce the large-
178 scale pattern of the observed rainfall associated with PCC 0.72 and 0.77 (Table 1) respectively
179 for JJAS 2003 and JJAS 2004 over the West Africa domain, despite some biases at the locale
180 scale. The spatial extent of rainfall maxima and the North-South gradient are well captured by
181 control experiments; however, their magnitudes are underestimate. In general, a dry mean bias
182 about -49.31% and -50.56% are found respectively for JJAS 2003 and JJAS 2004 over the
183 whole West African domain (Table 1). Figure 3 displays change in mean precipitation (in %)
184 for JJAS 2003 and JJAS 2004, for dry and wet experiments with respect to their corresponding
185 control experiments, the dotted area shows changes with statistical significance of 0.05 level.
186 The sensitivity dry and wet experiments show that precipitation has been significantly affected
187 by soil moisture anomalies at varying degrees according to the sub-regions (Fig. 3). In the dry
188 experiments (Fig.3a, c), we found a dominant decrease of rainfall over the central Sahel
189 especially in JJAS 2003 (Fig.3a), while the extent of this decrease is smaller in JJAS
190 2004(Fig.3c) and confined over the southern-west of Mali. On the other hand, we found a
191 dominant increase of rainfall over the Guinean coast and west Sahel, although there is a sparse
192 decrease, especially over the Guinea coast. In the wet experiments (Fig.3b, d), there is a
193 dominant increase of rainfall over most of the domains studied with a sparse decrease especially
194 along the coastline of Liberia, Sierra Leone and Guinea for both JJAS 2003 and JJAS 2004
195 (rep. Fig.3a and c). Overall, the impact on the precipitation of the anomalies in initial soil
196 moisture is homogeneous particularly over central Sahel, i.e, the dry (wet) experiments with
197 respect to the control exhibits significant decrease (increase) of precipitations (Fig.3a, b).



198 For a better quantitative evaluation, the PDF distributions of the changes in precipitation in
199 JJAS 2003 and JJAS 2004, over (a) central Sahel, (b) West Sahel, (c) Guinea coast and (d) West
200 Africa derived from dry and wet experiments compared to the corresponding control
201 experiments are shown in Figure 4. The impact on the precipitation of anomalies in initial soil
202 moisture is not homogeneous over most of the studied domains (Fig.4 b-d) except over central
203 Sahel where the dry (wet) experiments with respect to the control display significant decrease
204 (increase) of precipitation (Fig.4a.). However, the strongest impact on precipitation in wet and
205 dry experiments is found respectively over west and central Sahel, and the peak mode of change
206 is about respectively 40% and -8%. The impact on precipitation in wet experiment is stronger
207 than in dry experiment.

208 It is worth to note that, over the West Sahel and Guinea coast, for both dry and wet experiments
209 tend to cause an increase of precipitation. This indicates that the increase of precipitation is
210 more likely to happen not only in the wet experiment but also in the dry experiment (Fig. 4b).
211 The lag between the JJAS 2003 and JJAS 2004 PDFs for wet and dry experiments indicates a
212 somewhat significant impact when comparing the two years, particularly over Guinea and west
213 Sahel (Fig. 4 b and c). The wet year has a higher impact compared to the dry year over most of
214 domains studied (Fig. 4). These results are consistent with previous studies which supported a
215 strong relationship between precipitation and soil moisture in particular over the transition
216 zones with a climate between wet and dry climate regimes (Koster and al., 2004; Liu and al.,
217 2014; Douville and al., 2001).

218 To better study the influence of soil moisture anomalies on precipitation for the both dry and
219 wet years over the West African domain and its sub-regions, we analyzed changes in the daily
220 domain-average of soil moisture and precipitation (resp. Figure 5 and Figure 6) for JJAS 2003
221 and JJAS 2004, from dry and wet experiments with respect to their corresponding controls
222 experiments. The third soil layer in CLM4.5 (0 to 11.89 cm) is used in this study, this soil layer
223 corresponds almost to the top layer soil moisture used by Hong and al. (2000) in their work. In
224 general, soil moisture anomalies persist for three or four months over the domains studied
225 (Fig.5). The anomalies of soil moisture disappear for dry and wet experiments with varying
226 duration, between three to four months from one region to another over the domain studied.
227 The strongest duration and amplitude is found over the west Sahel sub-region, for the both wet
228 and dry experiments, it lasts four months in JJAS 2003 and JJAS 2004, although the signal is
229 rather weak in the wet experiments as compared to the dry ones (Fig. 5b). The weaker change
230 in soil moisture anomalies is found over the Guinea coast for wet experiments and lasts three



231 months (Fig. 5c). While in dry experiments, the weaker change in soil moisture anomalies is
232 found over central Sahel and last three months (Fig.5a).

233 Figure 6 shows response of the daily precipitation to the anomalies in initial soil moisture over
234 the different domains studied. In general, the impact of the wet soil moisture anomalies on daily
235 precipitation is larger in magnitude as compared to the dry anomalies over most of domains
236 studied (Fig. 6). The strongest daily precipitation response in dry experiment ($-4\text{mm}\cdot\text{day}^{-1}$) is
237 found over the Guinea coast in the wet year JJAS 2003 (Fig. 6c), while for the wet experiments
238 (more than $8\text{mm}/\text{day}$, especially in JJAS 2003), it is found over the West Sahel and the Guinea
239 coast (resp. Fig. 6 b and c). However, the impact on daily precipitation of the anomalies in
240 initial soil moisture is much shorter lived as compared to soil moisture change. The significant
241 impact on daily precipitation, greater than $1\text{mm}\cdot\text{day}^{-1}$ is shown only in wet experiment and last
242 no longer than fifteen days for most of domains studied, except for the Guinea coast where it
243 lasts about 1 month. It is worth to note the peaks in precipitation over West Sahel and Guinea
244 coast (resp. Fig.6b and c) during the two months August and September that coincide with
245 fluctuation in the anomalies of soil moisture (Fig.5b and c). This indicates the soil moisture and
246 precipitation feedback is strong during this period over Guinea coast and West Sahel regions.
247 The response of the daily precipitation to the anomalies in initial soil moisture is also sensitive
248 to the wet and dry year. This is indicated by the lag between dry and wet experiments for JJAS
249 2003 and JJAS 2004 years (Fig6). The magnitude of impacts due to contrasting years depends
250 on the place. For example, over Guinea coast, in the dry experiments, the wet year presents the
251 greater impact compared to the dry year (Fig.6 c). This trend is reversed for the central Sahel
252 (Fig. 6a). These results are in line with the previous works which argued that the soil moisture-
253 atmosphere feedback strength and the land memory depend on the place (Vinnikov et al. 1996;
254 Vinnikov and Yeserkepova 1991).

255 Figure 7 and 8 show the vertical profile change respectively in humidity and temperature for
256 JJAS 2003 and JJAS 2004 from the dry and wet experiments with respect to control experiments
257 over the whole West Africa domain and its sub-region indicated in Fig. 1.

258 For the dry and wet experiments, the impact on humidity and temperature (Fig. 7 and Fig. 8)
259 are significant in the lower troposphere. The dry (wet) soil moisture experiments, in the lower
260 and somewhat in the middle troposphere, show drying (moistening) and warming (cooling)
261 respectively for humidity and temperature, indicating weak (strong) dry convection over most
262 of the domains studied (Fig.7 and Fig.8). The strongest impact on humidity and temperature in
263 lower and middle troposphere is found over central Sahel (Fig. 7a and Fig. 8a). These results in
264 the lower troposphere are consistent with the precipitation sensitivity, especially over central



265 Sahel in JJAS 2003 (Fig.3 a, b). However, over west Sahel and the Guinea coast this impact is
266 somewhat weak as compared to central Sahel. In the dry experiments over the Guinea coast
267 (Fig. 7c), these trends are reversed above 500 hPa for humidity, indicating wet convection in
268 this sub-region. These results in the lower atmosphere are consistent with the precipitation
269 sensitivity over the Guinea coast (Fig.3a, c).

270 On the other hand, in the upper troposphere, the significant impact on humidity and temperature
271 is found only for wet experiments, and exhibits a drying and warming respectively for humidity
272 and temperature over all the domains studied (Fig.7 and Fig.8). In the wet experiments, the
273 impact on upper tropospheric variability of the anomalies in initial soil moisture is also
274 identified by Hong and Pal (2000). The effect of soil moisture anomalies is mostly confined to
275 the near-surface and somewhat in the upper troposphere.

276 For understanding of the origins of the precipitation changes in Figure 3, we analyzed the lower
277 tropospheric wind (850hpa) and moisture changes for JJAS 2003 and JJAS 2004 from the dry
278 and wet experiments with respect to their corresponding control experiments in Figure 9. In the
279 dry experiments, we found a dominant decrease of moistening over most of domain studied,
280 however the strong wind magnitude change over the Atlantic ocean, tends to bring the increase
281 of moistening from the ocean to Guinea coast and west Sahel, this can explain the increase of
282 precipitation over these sub-region in the dry experiments. While over the central Sahel, a weak
283 change in wind magnitude is found, leading to the strong decrease of precipitation there,
284 especially in JJAS 2003 (Fig.3a). On the other hand, in wet experiments, an increase in
285 moistening is located over most of domain studied. And the strong change in wind magnitude,
286 tend to bring the moistening from the North to South, leading to the increase of precipitation
287 observed over most of domain studied in wet experiments (Fig. 3 b and d). These results are
288 broadly consistent to the dry and wet precipitation changes shown in Figure 3.

289 Summarizing this section results, the anomalies in soil moisture anomalies persist for three or
290 four months, while the significant impact on precipitation, greater than $1\text{mm}\cdot\text{day}^{-1}$, of the
291 anomalies in soil moisture is much shorter, no longer than one month. The anomalies in initial
292 soil moisture effect are mostly confined to the near-surface climate and somewhat in the upper
293 troposphere.

294 **3.2. Influence on temperature and other surface fluxes.**

295 The spatial distribution of averaged temperature ($^{\circ}\text{C}$) from observations CRU (Fig.10 a and d)
296 and GTS (Fig.10 b and e) for JJAS 2003 and JJAS 2004 and their corresponding simulated from
297 control experiments (Fig.10 c and f) initialized with reanalysis soil moisture ERA20C is shown



298 in Fig.10. Table 2 resumes the PCC and the MB between the simulation of the temperatures
299 and CRU observation, calculated for west Sahel, central Sahel, Guinea coast and the whole
300 West African domain.

301 The CRU temperature displays a zonal distribution over the whole West Africa domain. The
302 maximum values about 34 °C are located over the Sahara, and the lowest temperatures are
303 found on the Guinea coast especially over the orographic regions such as Guinean highlands,
304 Cameroon mountains and the Jos Plateau, where the temperature not exceeding 26°C. The two
305 observation datasets GTS and CRU are similar at large spatial scale with PCC about 0.99 over
306 the entire West African domain for both JJAS 2003 and JJAS 2004 (Table 2). However, the
307 extension and the amplitude of these maxima and minima are quite different in the two sets of
308 gridded observations. While GTS (Fig.10b and e) observation displays large (small) areas with
309 maxima (minima) values, CRU (Fig.10a and d) has small (large) area of these maxima (minima)
310 values. The strongest mean warm biases between the two observation products, about 0.54°C
311 and 0.67°C respectively for JJAS 2003 and JJAS 2004, are located over the west Sahel sub-
312 region as compared to the other sub-regions (Table 2). The control experiments (Fig.10 c and
313 f) show a good agreement in representing the large-scale pattern of the observed temperature
314 (CRU) with PCC 0.99 for both JJAS 2003 and JJAS 2004 (Table 2), comprising the zone of the
315 meridional gradient of the surface temperature between Sahara Desert and Guinea coast which
316 is crucial for the African easterly jet (AEJ) evolution and formation (Thorncroft and Blackburn
317 1999; Cook 1999). However, some biases are noted at the local scale. The spatial extent of
318 temperature maxima and minima are well reproduced by control experiments, however their
319 magnitude are overestimate. The strongest warm mean biases of control experiments with
320 respect to CRU observation are about 2.68 °C and 2.14 °C respectively for JJAS 2003 and JJAS
321 2004, are found over the West Sahel sub-region (Table 2).

322 Figure 11 shows changes in mean temperature (°C) for JJAS 2003 and JJAS 2004, from dry
323 and wet experiments with respect to their corresponding control experiments. The dotted area
324 shows changes with that are statistical significance of 0.05 level. In the dry experiments, for
325 both JJAS 2003 and JJAS 2004, the dominant warm changes are located most the area under
326 the latitude 13°N, with maximum values located over the Guinea coast. However, a mixture of
327 warm and cool changes is located over the latitude 13°N (Fig.11a and c). On the other hand, for
328 the wet experiments, we found a dominant cool change over most of the area under the latitude
329 15°N, with maximum values around the latitude 13°N. While, a dominant warm change is
330 located above the latitude 15°N (Fig.11 b and d). Overall, the temperature is more sensitive to
331 soil moisture anomalies than precipitation over most of the domains studied.



332 For a better quantitative evaluation, the PDF distributions of the changes in mean temperature
333 in JJAS 2003 and JJAS 2004, over (a) central Sahel, (b) West Sahel, (c) Guinea and (d) West
334 Africa derived from dry and wet experiments compared to the corresponding control
335 experiments are shown in Figure 12. The temperature impact is homogeneous over central Sahel
336 and Guinea coast (Fig.12a and c). The strongest homogeneous impacts on temperature of the
337 anomalies in initial soil moisture is located over the central Sahel, i.e, the dry (wet) experiments
338 display a decrease (an increase) in temperature change with the peak mode of change at -1.5°C
339 (0.5°C) as compared to other sub-regions, for both JJAS 2003 and JJAS 2004. Over the west
340 Sahel, both wet and dry experiments lead to a decrease of temperature. The impact on
341 temperature of the anomalies in soil moisture is somewhat sensitive to the wet and dry year, as
342 mentioned above, it is indicated by the lag between wet and dry experiments (Fig. 12). The
343 impact on dry and wet years depends on the area and the type of experience dry or wet. Overall,
344 the dry (wet) sensitivity experiments for 2m-temperature show a dominant increase (decrease)
345 of warming (cooling) for both JJAS 2003 and JJAS 2004 over most of the domains studied
346 except west Sahel where both dry and wet experiments lead to an increase of temperature
347 (Fig.12).

348 We now analyze the influence of initial soil moisture anomalies on land energy balance,
349 particularly on the surface fluxes sensible and latent heat. Figure 13 shows changes in sensible
350 heat fluxes (in $\text{W}\cdot\text{m}^{-2}$) for JJAS 2003 and JJAS 2004, from dry and wet experiments compared
351 to their corresponding control experiments, and the dotted area shows changes with statistical
352 significance of 0.05 level. It can be seen in figure 13, the initial soil moisture anomalies strongly
353 affect the sensible fluxes.

354 In the dry experiments, the increase of sensible heat flux changes are located under the latitude
355 15°N , while the decrease of sensible heat flux changes are found over most of area above the
356 latitude 15°N for both JJAS 2003 and JJAS 2004 (Fig.13a, c). Conversely, in wet experiments
357 we have a dominant decrease of sensible heat flux changes, found over almost whole West
358 Africa domain except the orographic and somewhat along Guinea coastline for both JJAS 2003
359 and JJAS 2004 (see Fig 13b, d).

360 The PDF distributions of the change in sensible heat flux are displayed in Figure 14. The dry
361 (wet) experiments show an increase (decrease) of the sensible flux in both JJAS 2003 and JJAS
362 2004 over all the domains studied (Fig. 14). The impact in wet experiments is strong compared
363 to the dry experiments over central and west Sahel except over Guinea coast (Fig. 14). Overall,
364 the impact on sensible heat flux of soil moisture anomalies is homogeneous, i.e., dry
365 experiments tend to cause an increase of sensible heat flux while the wet experiments tend to



366 favor a decrease of sensible heat flux over all domains studied. The strongest impacts on
367 sensible heat flux in wet and dry experiments are found over respectively west Sahel and Guinea
368 coast, with peak modes about respectively $-40\text{W}\cdot\text{m}^{-2}$ and $10\text{W}\cdot\text{m}^{-2}$ (resp. Fig. 14,b and Fig. 14c).
369 Unlike to sensible heat case, changes in latent heat show opposite patterns, we found a dominant
370 decrease (increase) of latent heat flux in dry (wet) experiment over almost the studied domains.
371 Nevertheless, in the dry experiments, we found a sparse increase of latent heat over the Sahara
372 and Senegal (Fig.15b, d), while in wet experiment a sparse decrease is located over the Guinea
373 coast (Fig.15b, d). The PDF distributions of latent heat flux change are shown in Figure 15. It
374 can be seen, the impact on latent heat flux of soil moisture anomalies is homogeneous, i.e. dry
375 experiments lead to a decreasing in latent heat flux while the wet experiments lead to an
376 increasing in the latent heat flux over most of the domains studied. The strongest impact on
377 latent heat flux in wet and dry experiments are found over respectively west Sahel and Guinea
378 coast with peaks mode at $40\text{W}\cdot\text{m}^{-2}$ and $-15\text{W}\cdot\text{m}^{-2}$ (resp. Fig. 16 b and Fig. 16 c). Overall, the
379 impacts in wet experiments on latent and sensible heat flux are strong compared to the dry
380 experiments over most of the domains studied, except over Guinea coast (Fig. 16).

381 In order to know if most of the changes in energy go to evaporating water, or to heating the
382 environment, we analyze in Fig. 17 the changes in Bowen ratio for JJAS 2003 and JJAS 2004,
383 from dry and wet experiments with respect to their corresponding control experiments. The
384 dotted area displays differences with statistical significance of 0.05 level. The soil moisture
385 anomalies strongly affected the Bowen ratio. The dry experiments show a dominant increase of
386 evaporation energy (Bowen ratio value in the range $[0,1]$) under the latitude 15°N for both JJAS
387 2003 and JJAS 2004 (Fig.17a, c). However, above latitude 15°N we found mixture of increase
388 and decrease of energy for environment heating (Bowen ratio value more than ± 1) (Fig.17a, c).
389 For the wet experiments (Fig.17b, d), we found a dominant decrease of energy for environment
390 heating above the latitude 14°N (Bowen ratio less than -1), while under this latitude, we found
391 a mixture of decrease and increase of evaporation energy (Bowen ratio in the range $[-1; 1]$). As
392 expected, the areas where most of the changes in energy go to evaporating water are generally
393 coincident with temperature changes. The decrease (increase) in evaporation area coincides
394 with decrease (increase) of temperature change.

395 For a quantitative evaluation, the PDF distribution of the Bowen ratio is shown in Figure 18.
396 Over the Guinea coast, for both dry and wet experiments, most of energy go to evaporation with
397 decrease in Bowen ratio about, the dry (wet) experiments show an increase (decrease) of water
398 evaporation energy about 0.12 (-0.1) in both JJAS 2003 and JJAS 2004 (Fig. 18c).



399 On other hand, over the central Sahel (Fig. 18 a), for the dry and wet experiments, most of
400 energy goes to evaporation. The dry (wet) experiments more increase (decrease) the
401 evaporation energy with pic at 0.4 (-0.7) for both JJAS 2003 and JJAS 2004 over the central.
402 In contrary over west Sahel (Fig. 18b), in wet (dry) experiments, most of the energy goes to
403 heat the environment (to evaporation) with a decrease in Bowen ratio about -3 (-0.1).

404 We now examine the impact on the stability of planetary boundary layer (PBL) of the anomalies
405 in initial soil moisture. Soil moisture can influence rainfall by limiting evapotranspiration,
406 which affects the development of the daytime planetary boundary layer and thereby the
407 initiation and intensity of convective precipitation (Eltahir, 1998). Figure 19 shows the changes
408 in PBL (in m) for JJAS 2003 and JJAS 2004, from dry and wet experiments with respect to
409 their corresponding control experiments with dotted areas with statistical significance of 0.05
410 level. The soil moisture anomalies impact significantly the PBL. The dry experiments show an
411 increase of the PBL under the latitude 15°N, except a western part of west Sahel, while a
412 dominant decrease of PBL is shown above this latitude for both JJAS 2003 and JJAS 2004
413 (resp. Fig.19 a and c). For the wet experiments, a decrease of PBL is located over most of the
414 domains studied, however a sparse increase is found above the latitude 15°N. The PDF
415 distribution of PBL changes, computed over the area indicated in Figure1 is shown in Figure
416 20. The impact on PBL is homogeneous over most of the domains studied (Fig.20). The dry
417 (wet) experiments lead to an increase (decrease) of PBL for both JJAS 2003 and JJAS 2004
418 over most of the domains studied. The strongest impacts on PBL, in the wet and dry
419 experiments, are found over respectively the west Sahel and Guinea coast, about respectively -
420 300 m and 150m. There is a dry (wet) air above the area where there is increase (decrease) of
421 PBL, which results in warm (cool) and dry (moist) over most of the domains studied (see Fig.
422 7 and Fig. 8). These results are consistent with the work of Han and Pan 2003.

423 Summarizing the results of this section, simultaneously cooling (warming) of surface
424 temperature (wet experiments) should be associated with a smaller (greater) sensible heat flux,
425 greater (smaller) of latent heat and a smaller (greater) depth of the boundary layer over most of
426 domains studied. These results are consistent with previous work of Eltahir and al. (1998).
427 Furthermore, sensible and latent heat fluxes, Bowen ratio and PBL responses to the anomalies
428 in initial soil moisture are somewhat sensitive to the contrast of year and experiments (wet and
429 dry).

430

431



432 **4. Summary and conclusion**

433

434 The impact of the anomalies in initial soil moisture on the subsequent summer mean climate
435 over West Africa is explored using the RegCM4-CLM45. The results were established for two
436 summers, JJAS 2003 (wet year) and JJAS 2004 (dry year). The sensitivity studies have been
437 carried out on the West African domain, at a spatial resolution of 25 km × 25 km. The control
438 runs are initialized by the reanalysis soil moisture ERA20C. We initialized the initial soil
439 moisture at the wilting points and the field capacity for dry and wet experiments respectively.

440 The RegCM4.7 responses for precipitation simulation related to the anomalies in initial soil
441 moisture anomalies show a homogeneous impact in the transition zones with a climate between
442 wet and dry climate regimes over the central Sahel, i.e. dry (wet) experiments leading to
443 precipitation decreasing (increasing). The strongest impact on precipitation in wet and dry
444 experiments is found respectively over west and central Sahel, and the peak mode of change is
445 about respectively 40% and -8%. The impact on precipitation in wet experiment is strong than
446 in dry experiment. It is worth to note that, over the West Sahel and Guinea coast, both dry and
447 wet experiments tend to cause a dominant increase of precipitation. This indicates that the
448 increase of precipitation is more likely to happen not only in the wet experiments but also in
449 the dry experiments. However, the increase of precipitation shown in the dry experiments
450 results from the bringing of moistening from the ocean to the west Sahel and Guinea coast, an
451 indication that the internal physics of the regional model is important in determining the
452 model's surface climate. The soil moisture anomalies can persist up to three or even four
453 months, however the significant response of precipitation to the anomalies in initial soil
454 moisture is much shorter, no longer than one month. The effect of soil moisture anomalies is
455 mostly confined to the near-surface climate and somewhat in the upper troposphere.

456 The temperature is more sensitive to the anomalies in initial soil moisture as compared to
457 precipitation over most of the domains studied. The dry (wet) experiments for 2m-temperature
458 show a dominant increase (decrease) of warming (cooling) for both JJAS 2003 and JJAS 2004
459 over most of the domains studied. The strongest homogeneous impacts of initial soil moisture
460 anomalies on temperature is located over the central Sahel, i.e. the dry (wet) experiments
461 display a decrease (an increase) in temperature change with the peak mode of change at -1.5 °C
462 (0.5°C) as compared to other sub-regions, for both JJAS 2003 and JJAS 2004.



463 The impact on sensible and latent heat, the Bowen ratio and the PBL height of the anomalies in
464 initial soil moisture have been investigated in this study. We found that, simultaneously cooling
465 (warming) of surface temperature (wet experiments) is associated with a smaller (greater)
466 sensible heat flux, greater (smaller) of latent heat and a smaller (greater) depth of the boundary
467 layer over most of domains studied, with different magnitudes varying from one sub-region to
468 another. The strongest impacts on sensible heat in wet and dry experiments are found over
469 respectively west Sahel and Guinea coast, with peak modes about respectively -40W.m^{-2} and
470 10W.m^{-2} (resp. Fig. 14b and 14c). For latent heat, they are found over respectively west Sahel
471 and Guinea coast with peaks mode at 40W.m^{-2} and -15W.m^{-2} (resp. Fig. 16b and 16c). In wet
472 and dry experiments, the major impacts are found for the height of the PBL, over respectively
473 the west Sahel and Guinea coast, and about -300 m and 150m , respectively.

474 Furthermore, the impact of the anomalies in initial soil moisture on the Bowen ratio was
475 investigated to know if most of the changes in energy go to evaporating water, or to heating the
476 environment.

477 As expected, over the Guinea coast most of the changes in energy go to evaporation, the dry
478 (wet) experiments show an increase (decrease) of water evaporation energy in both JJAS 2003
479 and JJAS 2004. On other hand, over the central and west Sahel, for the dry and wet experiments,
480 most changes in energy respectively go to evaporation and to heat the environment.

481 We recognize that sensitivity of "dry" and "wet" experiments of initial soil moisture conducted
482 in this work, as in previous studies, were not supposed to simulate real climate since such
483 extremes are not current. However, these experiments can supply some estimation of the limits
484 of internal influence of soil moisture forcing. . To more complete this study, we will explore
485 the influence of the anomalies in initial soil moisture on climate extreme.

486 **Author contribution**

487 The authors declare to have no conflict of interest with this work. B. Koné and A. Diedhiou
488 fixed the analysis framework. B. Koné carried out all the simulations and figures production
489 according to the outline proposed by A. Diedhiou. B. Koné and A. Diedhiou, S. Anquetin and
490 A. Diawara worked on the analyses. All authors contributed to the drafting of this manuscript.

491 **Acknowledgements**

492 The research leading to this publication is co-funded by the NERC/DFID "Future Climate for
493 Africa" programme under the AMMA-2050 project, grant number NE/M019969/1 and by
494 IRD (Institut de Recherche pour le Développement; France) grant number UMR IGE
495 Imputation 252RA5.



496

497 **References:**

498

499 Beljaars A. C. M., Viterbo P. , Miller M. J., and Betts A. K.: The anomalous rainfall over the
500 United States during July 1993: Sensitivity to land surface parameterization and soil moisture
501 anomalies, *Mon. Weather Rev.*, 124(3), 362–382, doi:10.1175/1520-0493(1996)124<0362:
502 TAROTU>2.0.CO;2, 1996.

503

504 Bosilovich, M. G., and Sun W. Y.: Numerical simulations of the 1993 Midwestern flood: Land–
505 atmosphere interactions. *J. Climate*, 12, 1490–1505, 1999.

506

507 Cook K. H.: Generation of the African easterly jet and its role in determining West African
508 precipitation, *J. Climate*, 12, 1165–1184, [https://doi.org/10.1175/1520-0442](https://doi.org/10.1175/1520-0442(1999)012) (1999)012
509 <1165:GOTAEJ> 2.0.CO;2, 1999.

510

511 Danielson J.J., and Gesch D.B.: Global multi-resolution terrain elevation data 2010
512 (GMTED2010): U.S. Geological Survey Open-File Report 2011–1073, 26 p, 2011.

513

514 Dirmeyer P. A., Koster R. D., and Guo Z.: Do global models properly represent the feedback
515 between land and atmosphere?, *J. Hydrometeorol.*, 7(6), 1177–1198, doi:10.1175/JHM532.1,
516 2006.

517

518 Douville, F. Chauvin, and H. Broqua.: Influence of soil moisture on the Asian and African
519 monsoons. Part I: Mean monsoon and daily precipitation. *J. Climate*, 14, 2381–2403, 2001.

520

521 Eltahir E. A. B.: A soil moisture-rainfall feedback mechanism 1. Theory and observations,
522 *Water Resour. Res.*, 34, 765–776, doi:10.1029/97WR03499, 1998.

523

524 Emanuel K. A.: A scheme for representing cumulus convection in large-scale models. *Journal*
525 *of the Atmospheric Science* 48: 2313–2335, 1991.

526

527 Fan Y., and van den Dool H.: A global monthly land surface air temperature analysis for 1948
528 - present, *J. Geophys. Res.* 113, D01103, doi: 10.1029/2007JD008470, 2008.



- 529
- 530 Gao, X.-J., Shi, Y., and Giorgi, F.: Comparison of convective parameterizations in RegCM4
531 experiments over China with CLM as the land surface model, *Atmos. Ocean. Sci. Lett.*, 9, 246–
532 254, <https://doi.org/10.1080/16742834.2016.1172938>, 2016.
- 533
- 534 Giorgi F., Coppola E., Solmon F., Mariotti L., Sylla M. B., Bi X., Elguindi N., Diro G. T.,
535 Nair V., Giuliani G., Cozzini S., Guettler I., O'Brien T., Tawfik A., Shalaby A., Zakey A. S.,
536 Steiner A., Stordal F., Sloan L., and Brankovic C.: RegCM4: model description and
537 preliminary tests over multiple CORDEX domains, *Clim. Res.*, 52, 7–29,
538 <https://doi.org/10.3354/cr01018>, 2012.
- 539
- 540 Grell G., Dudhia J. and Stauffer D. R.: A description of the fifth generation Penn State/NCAR
541 Mesoscale Model (MM5), National Center for Atmospheric Research Tech Note NCAR/TN-
542 398+STR, NCAR, Boulder, CO, 1994.
- 543
- 544 Harris I., Jones P. D., Osborn T. J. and Lister D. H.: Updated high-resolution grids of monthly
545 climatic observations, *Int. J. Climatol.*, 34, 623–642, <https://doi.org/10.1002/joc.3711>, 2013.
- 546
- 547 Holtslag A., De Bruijn E., and Pan H. L.: A high resolution air mass transformation model for
548 short-range weather forecasting, *Mon. Weather Rev.*, 118, 1561–1575, 1990.
- 549
- 550 Hong S. Y. and Pan H. L.: Impact of soil moisture anomalies on seasonal, summertime
551 circulation over North America in a regional climate model. *J. Geophys. Res.*, 105 (D24), 29
552 625–29 634, 2000.
- 553
- 554 Huffman G. J., Adler R. F., Bolvin D. T., Gu G., Nelkin E. J., Bowman K. P., Hong Y, Stocker
555 E. F., and Wolff D. B.: The TRMM multisatellite precipitation analysis: quasi-global, multi-
556 year, combined-sensor precipitation estimates at fine scale, *J. Hydrometeorol.*, 8, 38-55, 2007.
- 557
- 558 Jaeger E. B., and Seneviratne S.I.: Impact of soil moisture-atmosphere coupling on European
559 climate extremes and trends in a regional climate model, *Clim. Dyn.*, 36(9-10), 1919-1939,
560 [doi:10.1007/s00382-010-0780-8](https://doi.org/10.1007/s00382-010-0780-8), 2011.
- 561



- 562 Kang S, Im E.-S. and Ahn J.-B.: The impact of two land-surface schemes on the
563 characteristics of summer precipitation over East Asia from the RegCM4 simulations *Int. J.*
564 *Climatol.* 34: 3986-3997, 2014.
- 565
- 566 Kiehl J., Hack J., Bonan G., Boville B., Breigleb B., Williamson D., Rasch P. ; Description of
567 the NCAR Community Climate Model (CCM3). National Center for Atmospheric Research
568 Tech Note NCAR/TN-420+STR, NCAR, Boulder, CO, 1996.
- 569
- 570 Kim Y. J., and Wang G. L.: Impact of initial soil moisture anomalies on subsequent
571 precipitation over North America in the Coupled Land-Atmosphere Model CAM3–CLM3, *J.*
572 *Hydrometeorol.*, 8(3), 513–533, doi:10.1175/JHM611.1, 2007.
- 573
- 574 Kirtman B.P., Schopf P. S.: Decadal Variability in ENSO Predictability and Prediction. *Journal*
575 *of Clim.* 11, 2804, 1998.
- 576
- 577 Koné B., Diedhiou A., N’datchoh E. T., Sylla M. B., Giorgi F., Anquetin S., Bamba A., Diawara
578 A., and Koba A. T.: Sensitivity study of the regional climate model RegCM4 to different
579 convective schemes over West Africa. *Earth Syst. Dynam.*, 9, 1261–1278.
580 <https://doi.org/10.5194/esd-9-1261-2018>, 2018.
- 581
- 582 Koster R. D., Dirmeyer P. A., Zhichang G., Bonan G., Chan E., Cox P., Gordon C. T., Kanae
583 S., Kowalczyk E., Lawrence D., Liu P., Lu C. H, Malyshev S., McAvaney B., Mitchell K,
584 Mocko D., Oki T., Oleson K., Pitman A., Sud Y. C. , Taylor C. M., Verseghy D., Vasic R.,
585 Xue Y., Yamada T.: Regions of strong coupling between soil moisture and precipitation,
586 *Science*, 305, 1138–1140, doi:10.1126/science.1100217, 2004.
- 587
- 588 Lawrence D.M., Oleson K.W., Flanner M.G., Thornton P.E., Swenson S.C., Lawrence P.J. ,
589 Zeng X., Yang Z.-L., Levis S., Sakaguchi K., Bonan G.B., and Slater A.G.:Parameterization
590 improvements and functional and structural advances in version 4 of the Community Land
591 Model. *J. Adv. Model. Earth Sys.* 3. DOI:10.1029/2011MS000045, 2011.
- 592
- 593 Liu D., Wang G. L., Mei R. , Yu Z. B. and Gu H. H.: Diagnosing the strength of land-atmosphere
594 coupling at sub-seasonal to seasonal time scales in Asia, *J. Hydrometeor.*, doi:10.1175/JHM-
595 D-13-0104.1, 2013.



596

597 Liu D., G. Wang R. Mei Z. Yu, and Yu M.: Impact of initial soil moisture anomalies on climate
598 mean and extremes over Asia, *J. Geophys. Res. Atmos.*, 119, 529–545,
599 doi:10.1002/2013JD020890, 2014.

600

601 Loveland, T. R., Reed, B. C., Brown, J. F., Ohlen, D. O., Zhu, J., Yang, L., and Merchant, J.
602 W.: Development of a global land cover characteristics database and IGBP DISCover from 1-
603 km AVHRR Data, *Int. J. Remote. Sens.*, 21, 1303–1330, 2000.

604

605 Oglesby R. J., and Erickson III D. J.: Soil moisture and the persistence of North American
606 drought. *J. Climate*, 2, 1362–1380, 1989.

607

608 Oglesby R. J., Marshall S. , Erickson III D. J., Roads J. O. and Robertson F. R.: Thresholds in
609 atmosphere-soil moisture interactions: Results from climate model studies. *J. Geophys.*
610 *Res.*, 107, 4244, doi:10.1029/2001JD001045, 2002.

611

612 Oleson K., Lawrence D. M., Bonan G. B., Drewniak B., Huang M., Koven C. D., Yang Z. -L.:
613 Technical description of version 4.5 of the Community Land Model (CLM) (No. NCAR/TN-
614 503+STR). doi:10.5065/D6RR1W7M, 2013.

615

616 Paeth H., Girmes R., Menz G. and Hense A.: Improving seasonal forecasting in the low
617 latitudes, *Mon. Weather Rev.*, 134, 1859-1879, 2006.

618

619 Pal J. S., Small E. E. and Elthair E. A.: Simulation of regional scale water and energy budgets:
620 representation of subgrid cloud and precipitation processes within RegCM, *J. Geophys. Res.*,
621 105, 29579–29594, 2000.

622

623 Pal J. S. and Elthair E. A. B.: Pathways relating soil moisture conditions to future summer
624 rainfall within a model of the land–atmosphere system. *J. Climate*, 14, 1227–1242, 2001.

625

626 Peterson T. C., Folland C., Gruba G., Hogg W. Mokssit A., Plummer N.: Report on the
627 activities of the working group on climate change detection and related rapporteurs 1998-2001.
628 Geneva (Switzerland): WMO Rep. WCDMP 47, WMO-TD 1071, 2001.

629



- 630 Nicholson S. E.: The West African Sahel: a review of recent studies on the rainfall regime and
631 its interannual variability, *Meteorology*, 453521, 32 p., <https://doi.org/10.1155/2013/453521>,
632 2013.
- 633 Nikulin G., Jones C., Samuelsson P., Giorgi F., Asrar G., Büchner M., Cerezo-Mota R.,
634 Christensen O. B., Déque M., Fernandez J., Hansler A., van Meijgaard E., Sylla M. B. and
635 Sushama L.: Precipitation climatology in an ensemble of CORDEX-Africa regional climate
636 simulations, *J. Climate*, 6057–6078, <https://doi.org/10.1175/JCLI-D-11-00375.1>, 2012.
637
- 638 Rasmusson E. M. and Carpenter T. H.: Variations in Tropical Sea Surface Temperature and
639 Surface Wind Fields Associated with the Southern Oscillation/El Niño. *Mon. Weather Rev.*
640 110, 354, 1982.
641
- 642 Reynolds, R. W. and Smith, T. M.: Improved global sea surface temperature analysis using
643 optimum interpolation, *J. Climate*, 7, 929–948, 1994.
644
- 645 Seager R., and Vecchi G. A.: Greenhouse warming and the 21st century hydroclimate of
646 southwestern North America. *Proc. Natl. Acad. Sci. USA*, 107, 21 277–21 282,
647 [doi:10.1073/pnas.0910856107](https://doi.org/10.1073/pnas.0910856107), 2010.
648
- 649 Simmons A. S., Uppala D. D. and Kobayashi S.: ERA-interim: new ECMWF reanalysis
650 products from 1989 onwards, *ECMWF Newsl.*, 110, 29–35, 2007.
651
- 652 Solmon F., Giorgi F., and Liousse C.: Aerosol modeling for regional climate studies:
653 application to anthropogenic particles and evaluation over a European/African domain, *Tellus*
654 B, 58, 51–72, 2006.
655
- 656 Sundqvist H. E., Berge E., and Kristjansson J. E.: The effects of domain choice on summer
657 precipitation simulation and sensitivity in a regional climate model, *J. Climate*, 11, 2698-2712,
658 1989.
659
- 660 Thorncroft, C. D. and Blackburn, M.: Maintenance of the African easterly jet, *Q. J. R. Meteorol*
661 *Soc.*, 125, 763–786, 1999.
662



- 663 Uppala S., Dee D., Kobayashi S., Berrisford P. and Simmons A.: Towards a climate data
664 assimilation system: status update of ERA-interim, *ECMWF Newsl.*, 15, 12–18, 2008.
- 665
- 666 Vinnikov K. Y. and Yeserkepova I. B.: Soil moisture: Empirical data and model results, *J.*
667 *Clim.*, 4(1), 66–79, doi:10.1175/1520-0442(1991)004<0066:SMEDAM>2.0.CO;2, 1991.
- 668
- 669 Vinnikov K. Y., Robock A., Speranskaya N. A. and Schlosser A.: Scales of temporal and
670 spatial variability of midlatitude soil moisture, *J. Geophys. Res.*, 101(D3), 7163–7174,
671 doi:10.1029/95JD02753, 1996.
- 672
- 673 Wang, G., Yu, M., Pal, J. S., Mei, R., Bonan, G. B., Levis, S., and Thornton, P. E.: On the
674 development of a coupled regional climate vegetation model RCM-CLM-CN-DV and its
675 validation its tropical Africa, *Clim. Dynam.*, 46, 515–539, 2016.
- 676
- 677 Xue Y., De Sales F., Lau K. M. W., Bonne A., Feng J., Dirmeyer P., Guo Z., Kim K. M., Kitoh
678 A., Kumar V., Pocard-Leclercq I., Mahowald N., Moufouma-Okia W., Pegion P., Rowell D.
679 P., Schemm J., Schulbert S., Sealy A., Thiaw W. M., Vintzileos A., Williams S. F. and Wu M.
680 L.: Intercomparison of West African Monsoon and its variability in the West African Monsoon
681 Modelling Evaluation Project (WAMME) first model Intercomparison experiment, *Clim.*
682 *Dynam.*, 35, 3–27, <https://doi.org/10.1007/s00382-010-0778-2>, 2010.
- 683
- 684 Zakey A. S., Solmon F., and Giorgi F.: Implementation and testing of a desert dust module in
685 a regional climate model, *Atmos. Chem. Phys.*, 6, 4687–4704, [https://doi.org/10.5194/acp-6-](https://doi.org/10.5194/acp-6-4687-2006)
686 4687-2006, 2006.
- 687
- 688 Zeng X., Zhao M. and Dickinson R. E.: Intercomparison of bulk aerodynamic algorithms for
689 the computation of sea surface fluxes using TOGA COARE and TAO DATA, *J. Climate*, 11,
690 2628-2644, 1998.
- 691 Zhang, J., W.-C. Wang, and J. Wei, Assessing land-atmosphere coupling using soil moisture
692 from the Global Land Data Assimilation System and observational precipitation, *J. Geophys.*
693 *Res.*, 113, D17119, doi:10.1029/2008JD009807, 2008.



694 Zhang, J., W.-C. Wang, and L. R. Leung.: Contribution of land-atmosphere coupling to summer
695 climate variability over the contiguous United States, *J. Geophys. Res.*, 113, D22109,
696 doi:10.1029/2008JD010136, 2008.

697

698 Zhang, J. Y., L. Y. Wu, and W. Dong.: Land-atmosphere coupling and summer climate
699 variability over East Asia, *J. Geophys. Res.*, 116, D05117, doi 10.1029/2010JD014714, 2011.

700

701

702

703

704

705

706

707

708

709

710

711

712

713

714

715

716

717

718

719

720

721

722

723

724

725

726



727 **Tables and figures:**

728

	Central Sahel		West Sahel		Guinea		West Africa	
	PCC	MB (%)	PCC	MB (%)	PCC	MB (%)	PCC	MB (%)
TRMM 2003	0.98	7.60	0.96	-945	0.98	-15.45	0.97	-0.57
CTRL_2003	0.98	-47.97	0.87	-75.76	0.82	-47.12	0.73	-49.31
TMM 2004	0.98	-0.62	0.99	-7.03	0.98	-16.96	0.97	-1.56
CTRL_2004	0.98	-47.89	0.87	-68.35	0.85	-51.97	0.77	-50.56

729

730 **Table1:** The pattern correlation coefficient (PCC) and the mean bias (MB) for JJAS
 731 precipitation for model simulation and observation TRMM with respect to CHIRPS, calculated
 732 for Guinea coast, central Sahel, west Sahel and the entire West African domain during the
 733 period 2003 and 2004.

734

735

736

737

738

739

740

741

742

743

744

745



746

	Central Sahel		West Sahel		Guinea		West Africa	
	PCC	MB (°C)	PCC	MB (°C)	PCC	MB (°C)	PCC	MB (°C)
GTS 2003	0.99	0.31	0.99	0.54	0.99	0.28	0.99	0.39
CTRL_2003	0.99	1.52	0.99	2.68	0.99	-0.34	0.99	0.85
GTS 2004	0.99	0.32	0.99	0.67	0.99	0.28	0.99	0.40
CTRL_2004	0.99	1.50	0.99	2.14	0.99	-0.57	0.99	0.51

747

748 **Table2:** The pattern correlation coefficient (PCC) and the mean bias (MB) for JJAS 2m-
749 temperature for model simulation and observation (GTS) with respect to CRU, calculated for
750 Guinea coast, central Sahel, west Sahel and the entire West African domain during the period
751 2003 and 2004.

752

753

754

755

756

757

758

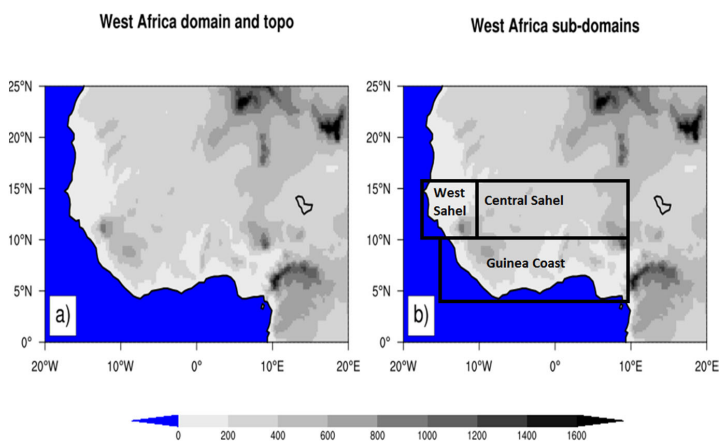
759

760

761

762

763



764

765

766 **Figure 1:** Topography of the West African domain. The analysis of the model result has an
767 emphasis on the whole West African domain and the three subregions Guinea coast, central
768 Sahel and west Sahel, which are marked with black boxes.

769

770

771

772

773

774

775

776

777

778

779

780

781

782

783

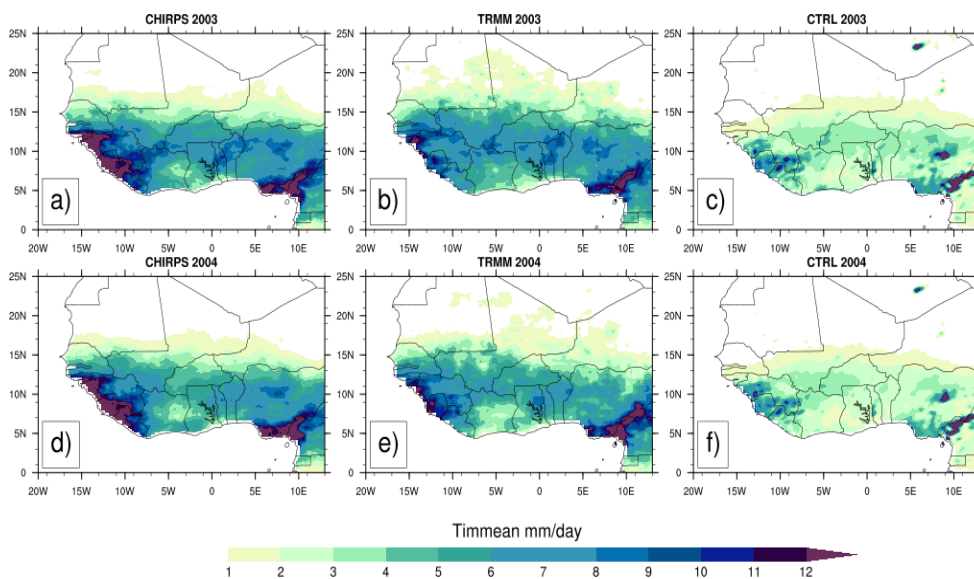
784

785

786

787

788



789

790

791 **Figure2:** Observed 4-month averaged (JJAS) precipitation (mm/day) from CHIRPS (a and d)

792 and TRMM (b and e) for 2003 and 2004 and their corresponding simulated control experiments

793 (CTRL) (c and f) with the reanalysis initial soil moisture ERA20C.

794

795

796

797

798

799

800

801

802

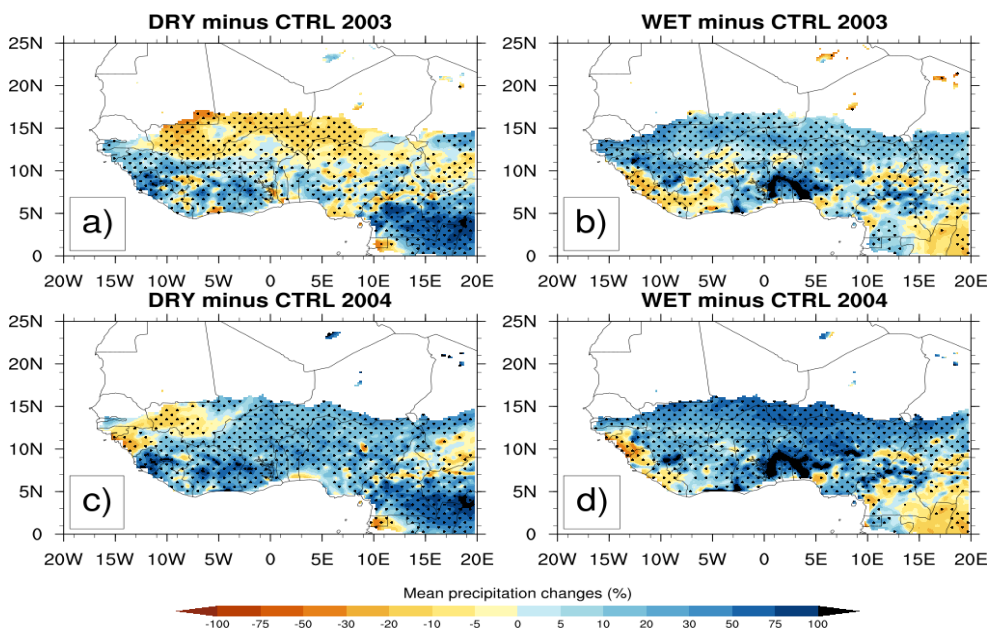
803

804

805

806

807



808

809

810 **Figure3:** Changes in mean precipitation (in %) for JJAS 2003 and JJAS 2004, from dry (resp.
811 a and c) and wet (resp. b and d) experiments with respect to their corresponding control
812 experiment, the dotted area shows differences that are statistically significant at 0.05 level.

813

814

815

816

817

818

819

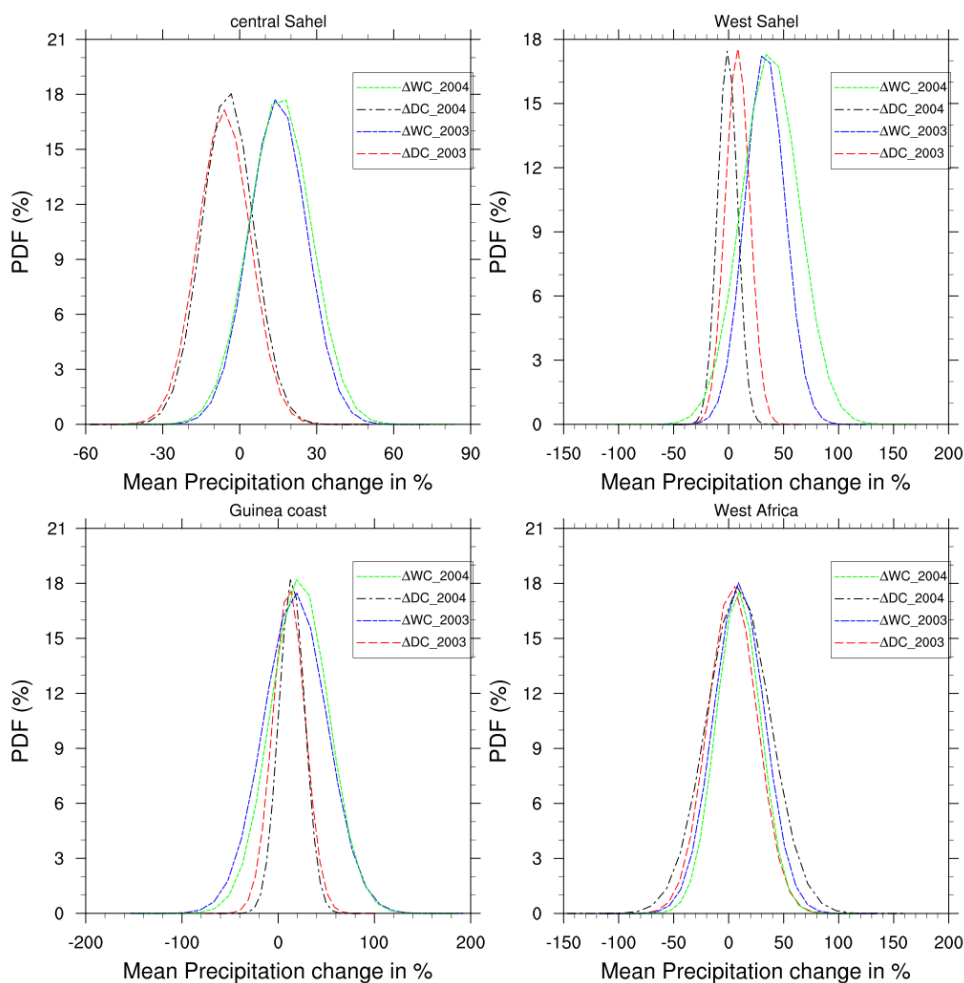
820

821

822

823

824



825

826

827 **Figure 4:** PDF distributions (%) of mean precipitation changes in JJAS 2003 and JJAS 2004,

828 over (a) central Sahel, (b) West Sahel, (c) Guinea and (d) West Africa derived from dry (DC)

829 and wet (WC) experiments compared to their corresponding control experiment.

830

831

832

833

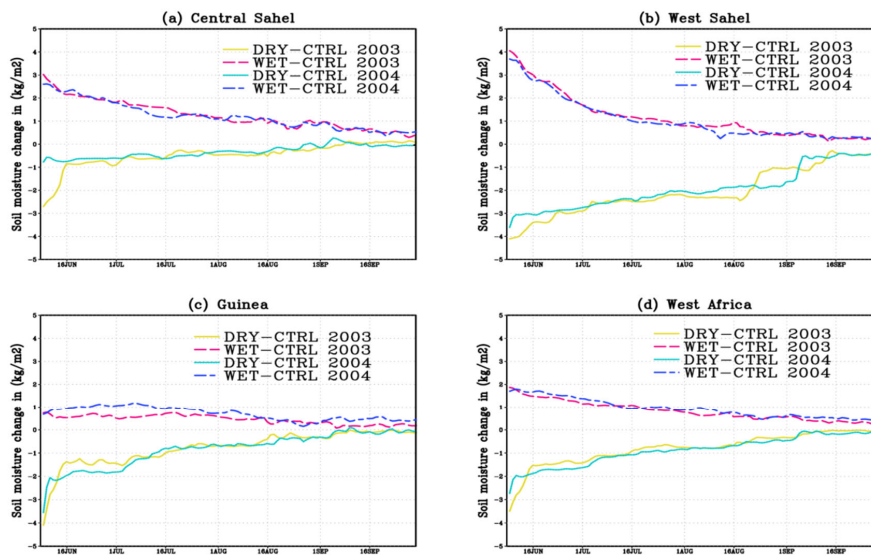
834

835

836



837



838

839 **Figure 5:** Daily domain-average soil moisture changes for JJAS 2003 and JJAS 2004, from dry
840 (a and c) and wet (b and d) experiments with respect to their corresponding control experiment.

841

842

843

844

845

846

847

848

849

850

851

852

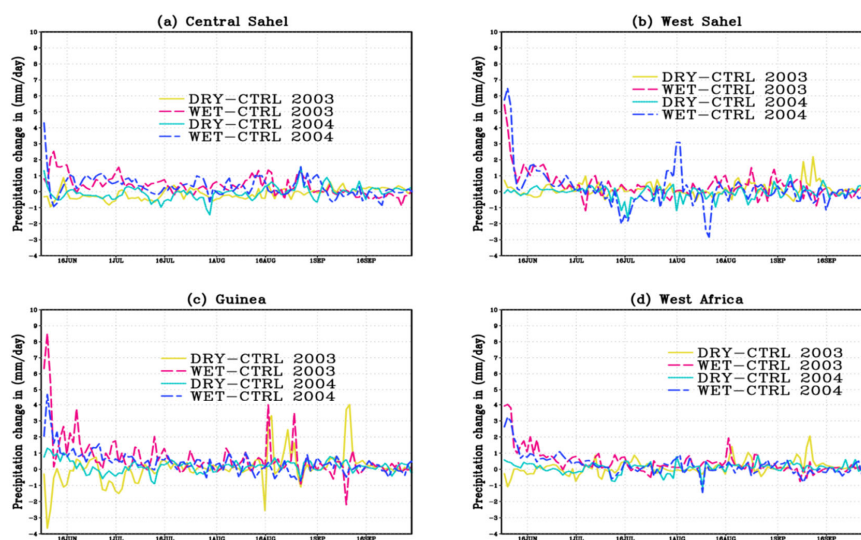
853

854

855

856

857



858

859

860 **Figure 6:** Daily domain-average precipitation changes for JJAS 2003 and JJAS 2004, from dry

861 (a and c) and wet (b and d) experiments with respect to their corresponding control experiment.

862

863

864

865

866

867

868

869

870

871

872

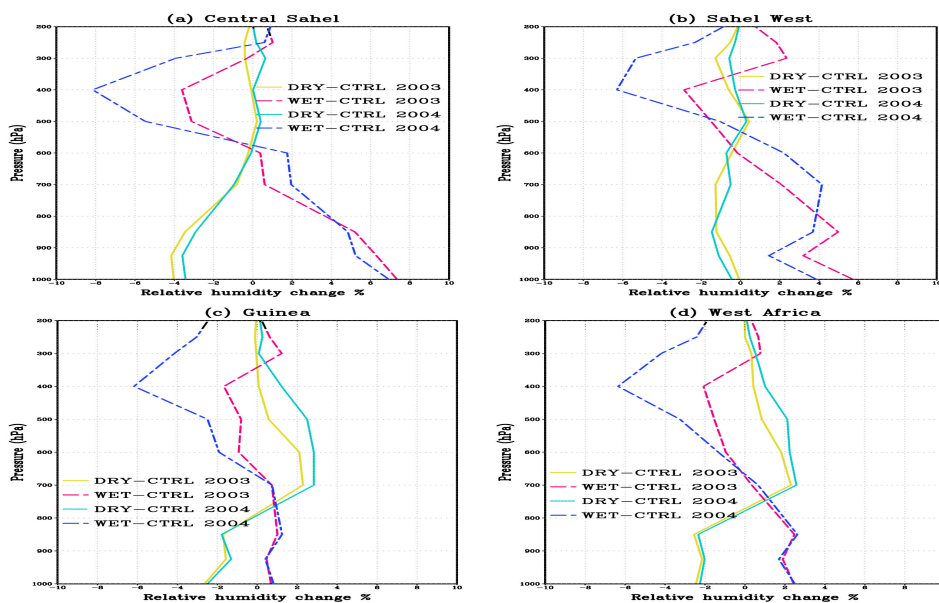
873

874

875

876

877



878

879 **Figure 7:** Vertical profile changes in humidity for JJAS 2003 and JJAS 2004 from the dry and
880 wet experiments with respect to corresponding control experiment over (a) central Sahel, (b)
881 west Sahel, (c) Guinea coast, and (d) West Africa.

882

883

884

885

886

887

888

889

890

891

892

893

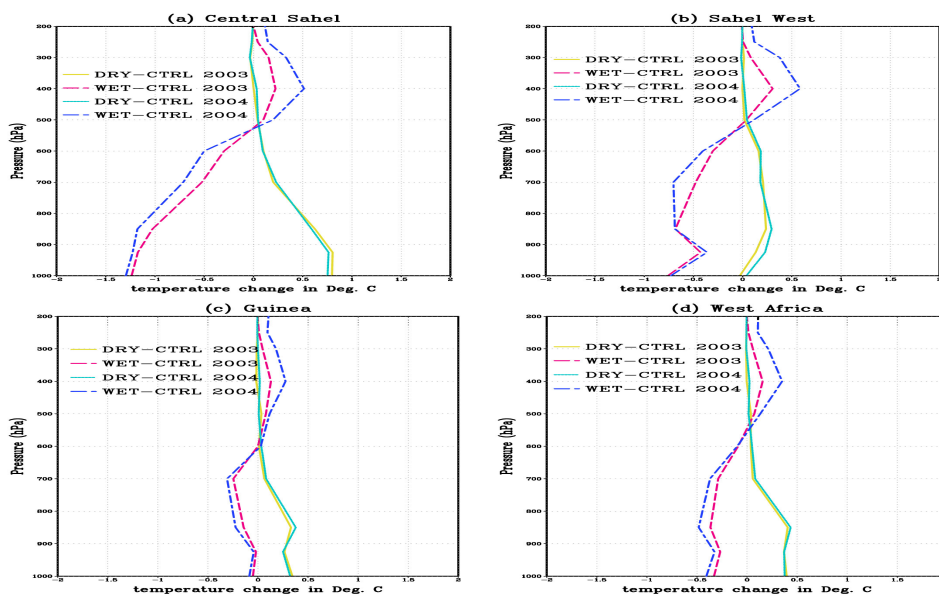
894

895

896

897

898



899

900 **Figure 8:** Vertical profile changes in temperature for JJAS 2003 and JJAS 2004 from the dry
901 and wet experiments with respect to their corresponding control experiment over (a) central
902 Sahel, (b) west Sahel, (c) Guinea coast, and (d) West Africa.

903

904

905

906

907

908

909

910

911

912

913

914

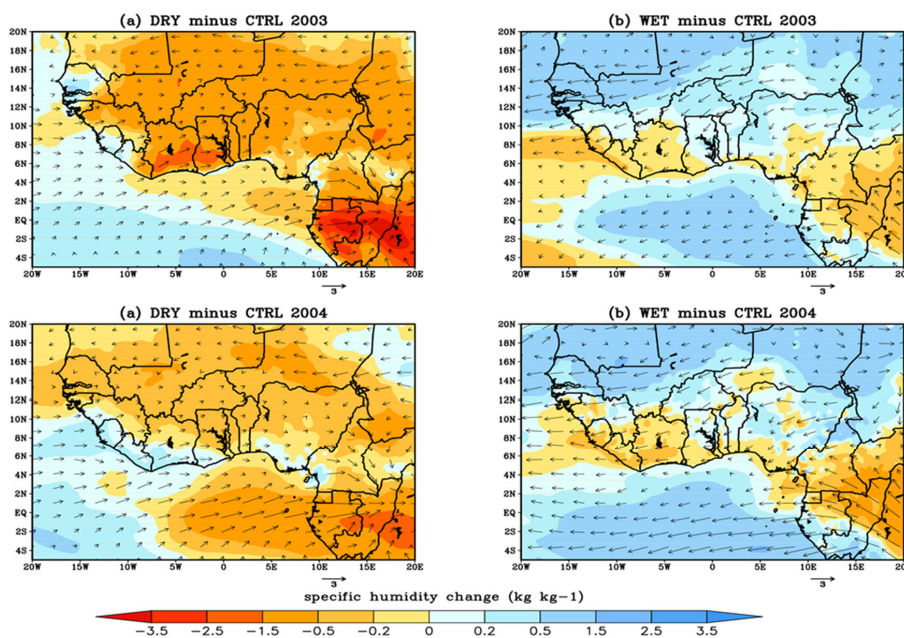
915

916

917

918

919



920

921 **Figure 9:** The lower tropospheric wind (850hpa) and moisture bias for JJAS 2003 and JJAS
922 2004 from the dry (a and c) and wet (b and d) experiments with respect to their corresponding
923 control experiment.

924

925

926

927

928

929

930

931

932

933

934

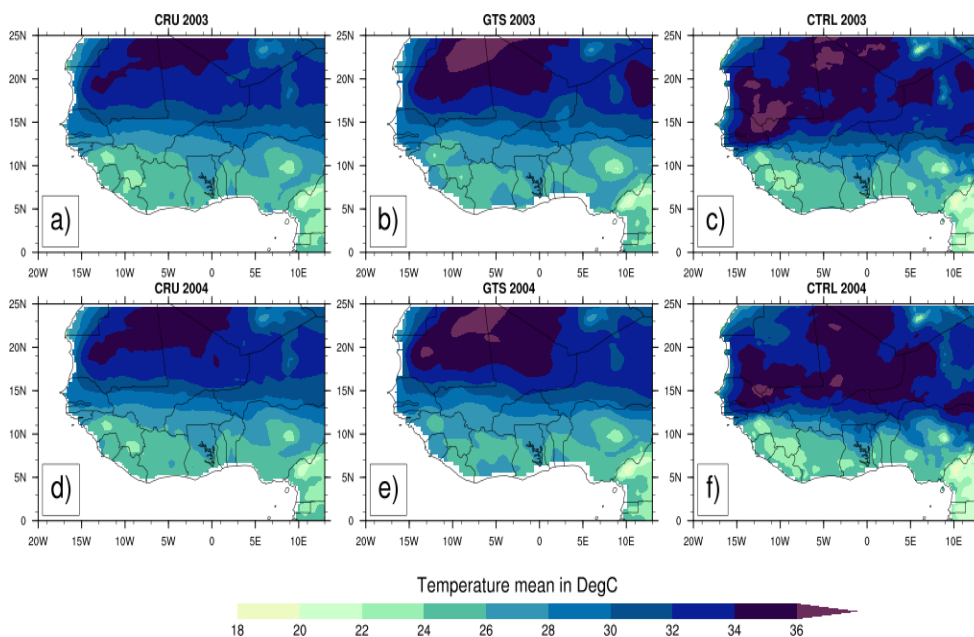
935

936

937

938

939



940

941

942 **Figure 10:** Observed 4-month averaged (JJAS) 2m-temperature (°C) from CRU (a and d) and

943 GTS (b and e) for 2003 and 2004 and their corresponding simulated control experiment (c and

944 f) with the reanalysis initial soil moisture ERA20C.

945

946

947

948

949

950

951

952

953

954

955

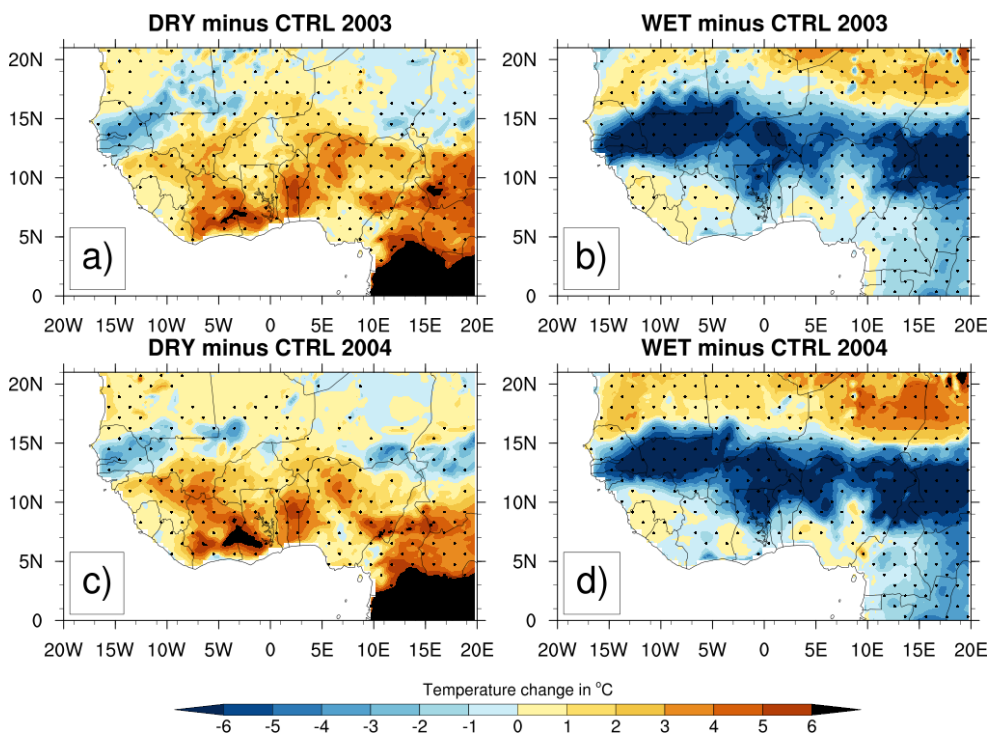
956

957

958

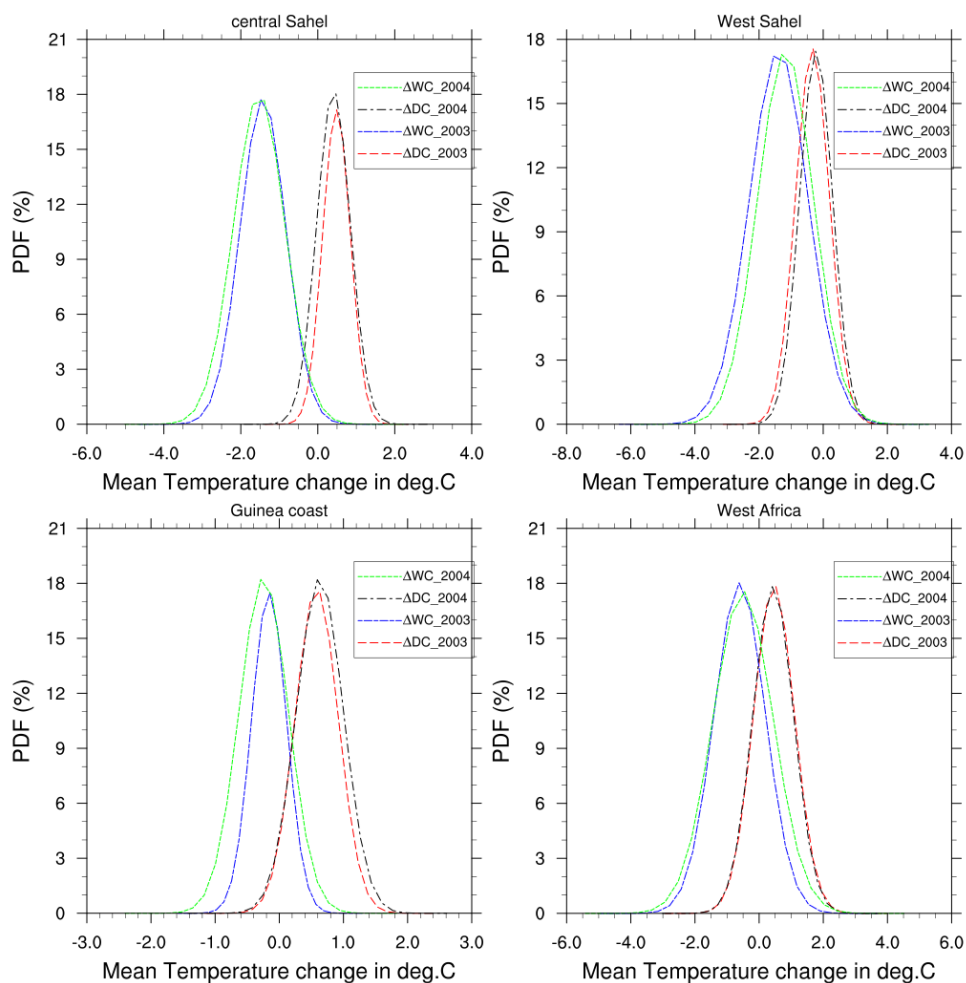
959

960



961
962
963
964
965
966
967
968
969
970
971
972
973
974
975
976
977
978
979

Figure 11: Changes in 2m-temperature (°C) for JJAS 2003 and JJAS 2004, from dry (resp. a and c) and wet (resp. b and d) experiments with respect to their corresponding control experiment, the dotted area shows differences that are statistically significant at 0.05 level.



980

981

982 **Figure 12:** PDF distributions (%) of mean temperature changes in JJAS 2003 and JJAS 2004,
983 over (a) central Sahel , (b) West Sahel, (c) Guinea and (d) West Africa derived from dry and
984 wet experiments compared to their corresponding control experiment.

985

986

987

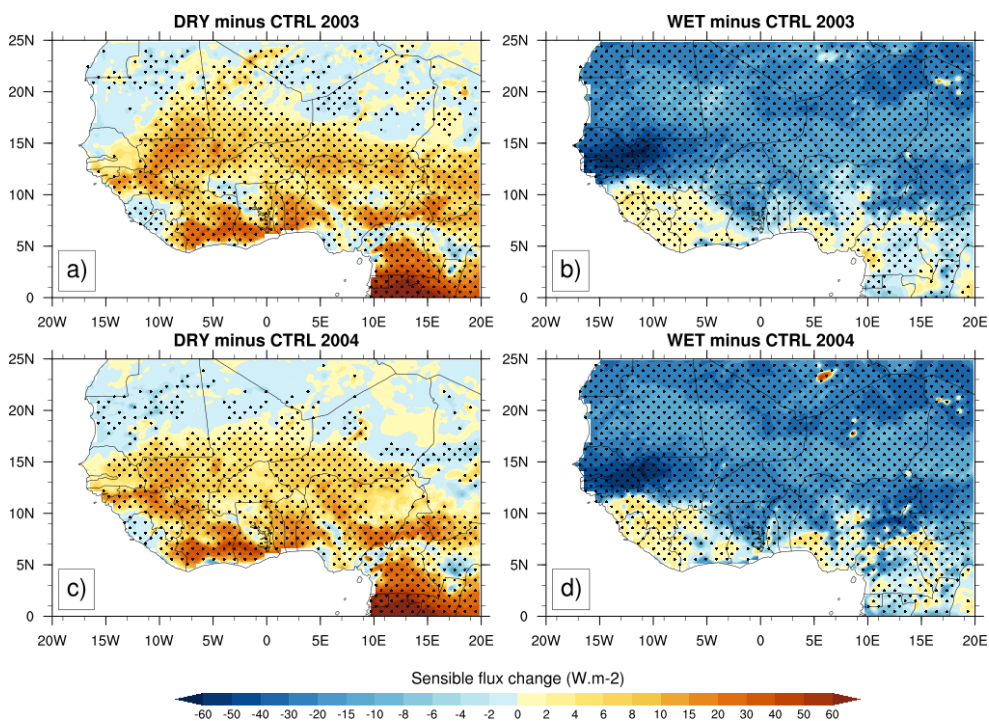
988

989

990

991

992



993

994

995 **Figure 13:** Same as Fig.11 but for sensible heat fluxes (in W.m⁻²).

996

997

998

999

1000

1001

1002

1003

1004

1005

1006

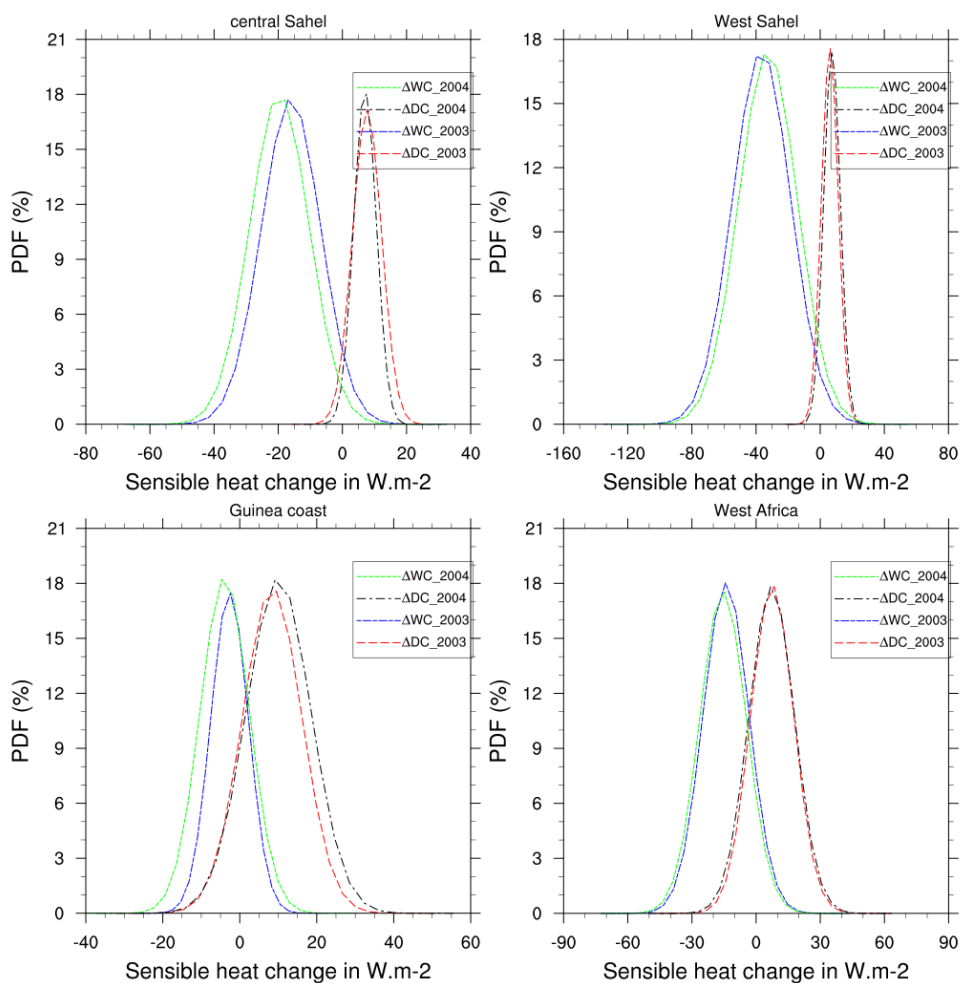
1007

1008

1009

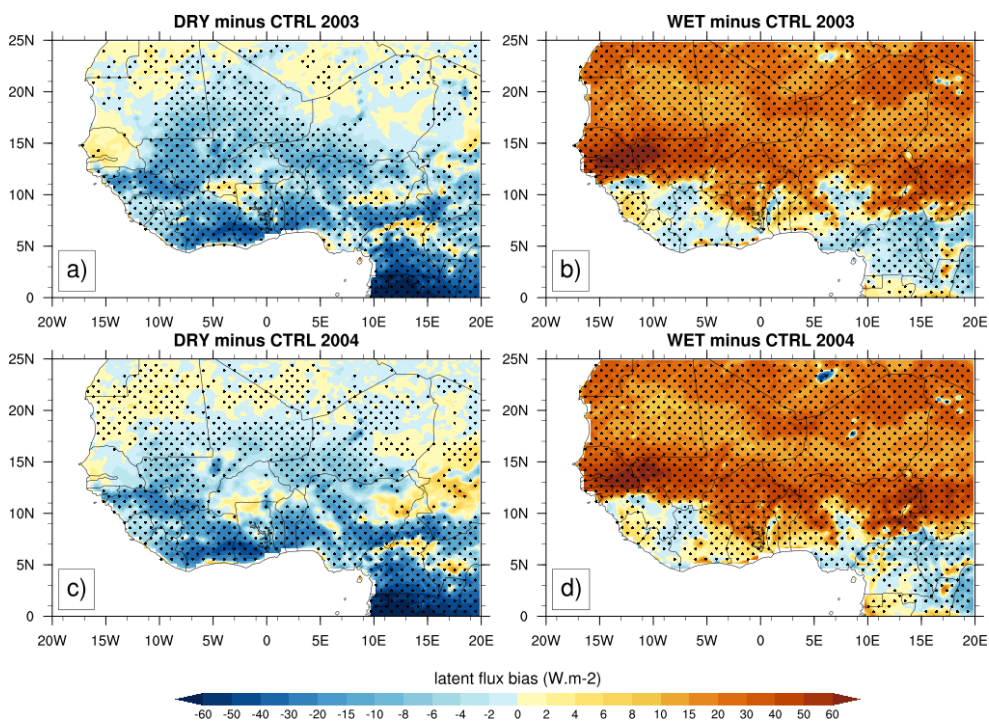
1010

1011



1012
1013
1014
1015
1016
1017
1018
1019
1020
1021
1022
1023
1024

Figure 14: Same as Fig.12 but for sensible heat fluxes (in $W.m^{-2}$).



1025

1026

1027 **Figure 15:** Same as Fig.11 but for latent heat fluxes (in $\text{W}\cdot\text{m}^{-2}$).

1028

1029

1030

1031

1032

1033

1034

1035

1036

1037

1038

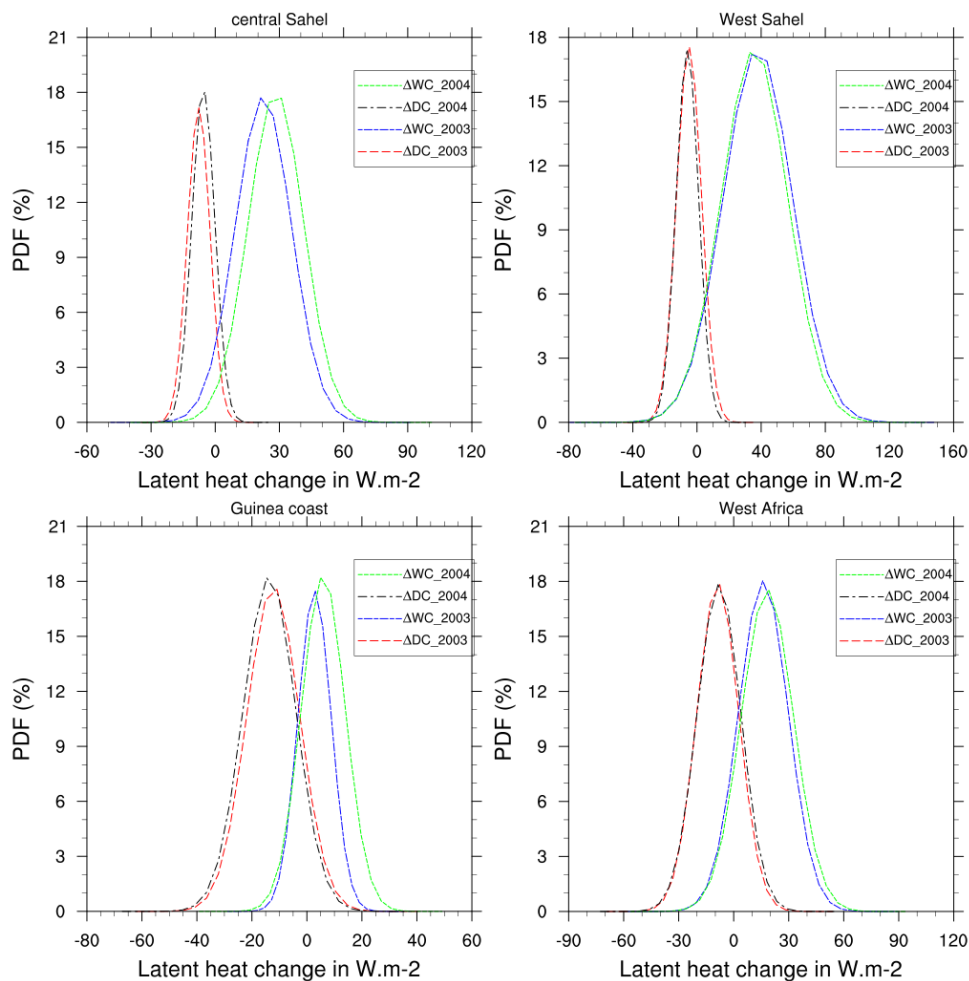
1039

1040

1041

1042

1043



1044

1045

1046 **Figure 16:** Same as Fig.12 but for latent heat fluxes (in W.m^{-2}).

1047

1048

1049

1050

1051

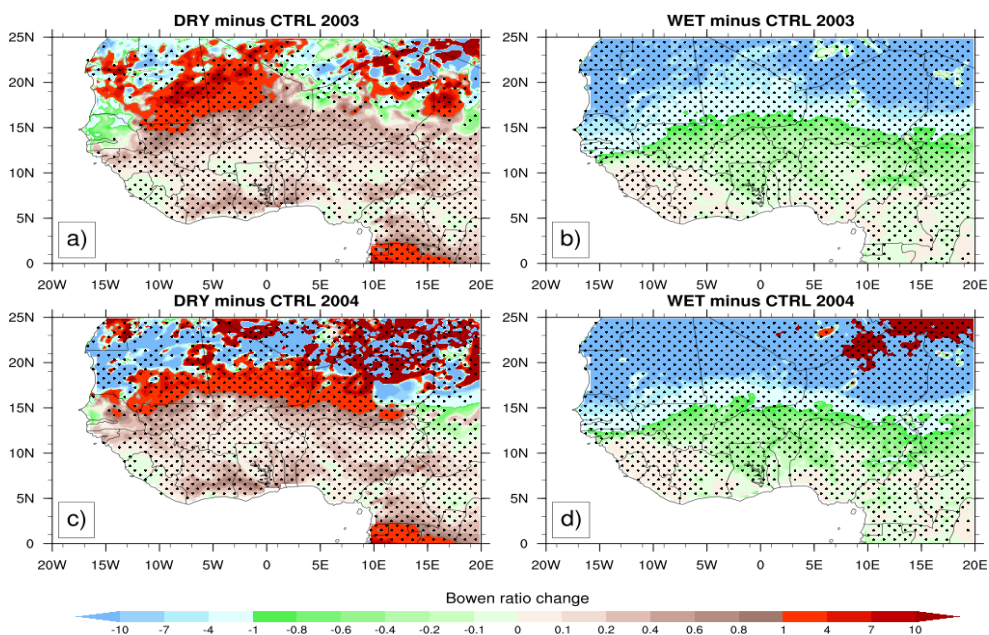
1052

1053

1054

1055

1056



1057

1058

1059 **Figure 17:** Same as Fig.11 but for Bowen ratio.

1060

1061

1062

1063

1064

1065

1066

1067

1068

1069

1070

1071

1072

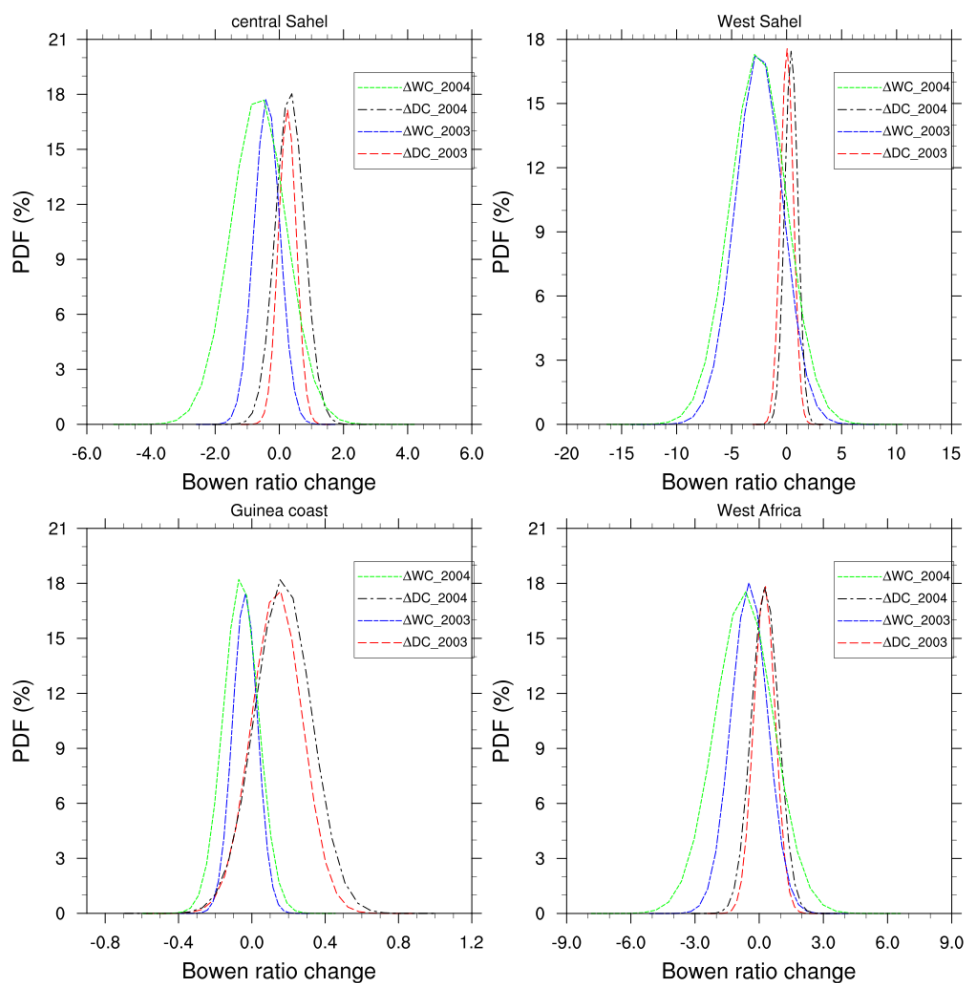
1073

1074

1075

1076

1077



1078

1079

1080 **Figure 18:** Same as Fig.12 but for Bowen ratio.

1081

1082

1083

1084

1085

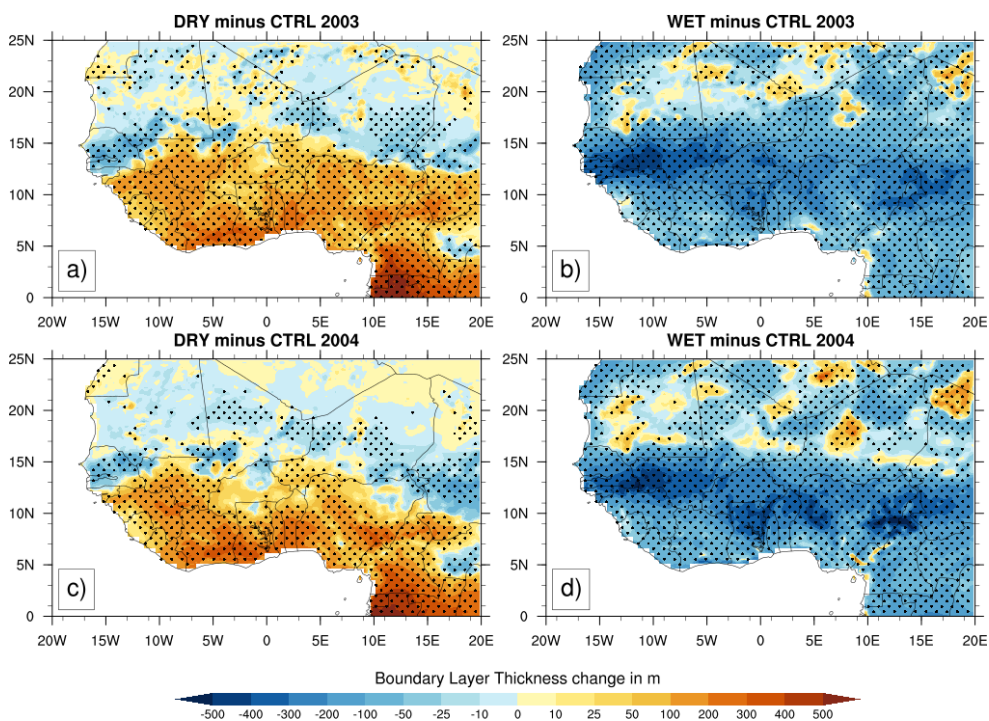
1086

1087

1088

1089

1090



1091

1092

1093 **Figure 19:** Same as Fig.11 but for the change of the height of the planetary boundary layer (in

1094 m).

1095

1096

1097

1098

1099

1100

1101

1102

1103

1104

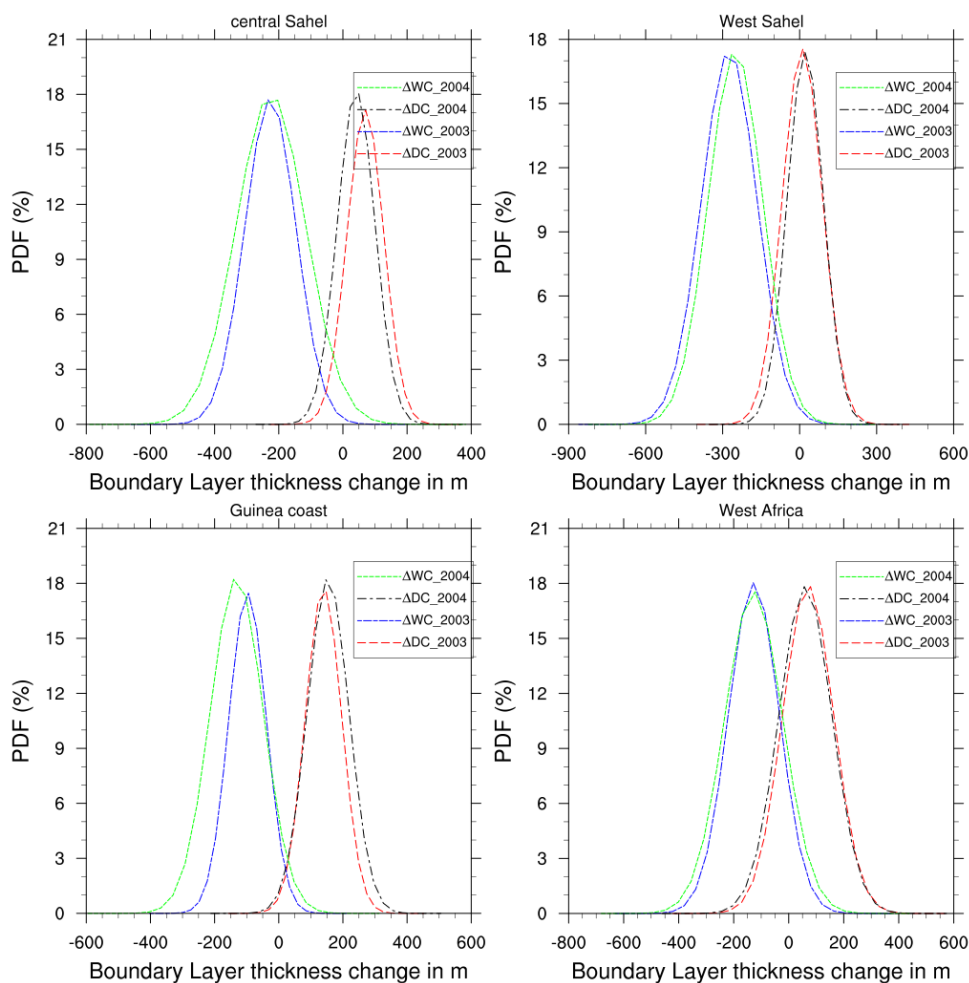
1105

1106

1107

1108

1109



1110

1111

1112 **Figure 20:** Same as Fig.12 but for the height of the planetary boundary layer (in m).

1113

1114

1115

1116

1117

1118

1119